



# Cometary plasma science

## Open science questions for future space missions

C. Goetz<sup>1,2</sup> · H. Gunell<sup>3</sup> · M. Volwerk<sup>4</sup> · A. Beth<sup>5</sup> · A. Eriksson<sup>6</sup> · M. Galand<sup>5</sup> · P. Henri<sup>7</sup> · H. Nilsson<sup>8</sup> · C. Simon Wedlund<sup>4</sup> · M. Alho<sup>9</sup> · L. Andersson<sup>10</sup> · N. Andre<sup>11</sup> · J. De Keyser<sup>12</sup> · J. Deca<sup>10</sup> · Y. Ge<sup>13</sup> · K.-H. Glassmeier<sup>14</sup> · R. Hajra<sup>15</sup> · T. Karlsson<sup>16</sup> · S. Kasahara<sup>17</sup> · I. Kolmasova<sup>18,19</sup> · K. LLera<sup>20</sup> · H. Madanian<sup>20</sup> · I. Mann<sup>21</sup> · C. Mazelle<sup>11</sup> · E. Odelstad<sup>16</sup> · F. Plaschke<sup>4</sup> · M. Rubin<sup>22</sup> · B. Sanchez-Cano<sup>23</sup> · C. Snodgrass<sup>24</sup> · E. Vigren<sup>6</sup>

Received: 28 July 2020 / Accepted: 9 July 2021 / Published online: 07 August 2021  
© The Author(s), under exclusive licence to Springer Nature B.V. 2021

### Abstract

Comets hold the key to the understanding of our Solar System, its formation and its evolution, and to the fundamental plasma processes at work both in it and beyond it. A comet nucleus emits gas as it is heated by the sunlight. The gas forms the coma, where it is ionised, becomes a plasma, and eventually interacts with the solar wind. Besides these neutral and ionised gases, the coma also contains dust grains, released from the comet nucleus. As a cometary atmosphere develops when the comet travels through the Solar System, large-scale structures, such as the plasma boundaries, develop and disappear, while at planets such large-scale structures are only accessible in their fully grown, quasi-steady state. In situ measurements at comets enable us to learn both how such large-scale structures are formed or reformed and how small-scale processes in the plasma affect the formation and properties of these large scale structures. Furthermore, a comet goes through a wide range of parameter regimes during its life cycle, where either collisional processes, involving neutrals and charged particles, or collisionless processes are at play, and might even compete in complicated transitional regimes. Thus a comet presents a unique opportunity to study this parameter space, from an asteroid-like to a Mars- and Venus-like interaction. The Rosetta mission and previous fast flybys of comets have together made many new discoveries, but the most important breakthroughs in the understanding of cometary plasmas are yet to come. The Comet Interceptor mission will provide a sample of multi-point measurements at a comet, setting the stage for a multi-spacecraft mission to accompany a comet on its journey through the Solar System. This White Paper,

---

✉ C. Goetz  
charlotte.goetz@esa.int

submitted in response to the European Space Agency's Voyage 2050 call, reviews the present-day knowledge of cometary plasmas, discusses the many questions that remain unanswered, and outlines a multi-spacecraft European Space Agency mission to accompany a comet that will answer these questions by combining both multi-spacecraft observations and a rendezvous mission, and at the same time advance our understanding of fundamental plasma physics and its role in planetary systems.

**Keywords** Comet · Plasma · Rosetta

## 1 Present day knowledge

At a comet there are two ion types: (1) the light solar wind ions, and (2) the cometary plasma, which usually consists of heavy ions that are produced from the ionisation of the neutral gas that surrounds a comet nucleus. As the neutral gas (called the *coma*) is not gravitationally bound due to the small size of the nucleus (100 m to 100 km), the neutrals and ions have a small radial velocity. Unhindered they would expand indefinitely into the near-vacuum of space. However, [14] found that the interaction of the cometary ions with the solar wind could accelerate them and form the plasma tail structures that are observable, sometimes even by eye, from Earth.

Comets can behave similarly to Mars and Venus in their **interaction with the solar wind**, since at both those planets the main obstacle is the conductive atmosphere and not the planets themselves nor their magnetic fields. This is also the case at comets, although there are significant differences in the outgassing speeds due to the much larger gravity of terrestrial planets and obstacle size difference.

The interaction of the two different types of plasma, protons from the solar wind and usually water or carbon dioxide ions from the comet, has been an object of studies for many years now. The spacecraft encounters with comets 21P/Giacobini-Zinner (21P) and 1P/Halley (1P) in the 1980s heralded the advent of modern cometary plasma science [128]. Beforehand, only remote observations were available. The golden age of cometary plasma science began with the arrival of the Rosetta spacecraft, in 2014, at comet 67P/Churyumov-Gerasimenko (67P, [56]). Rosetta was the first spacecraft to orbit a comet and take detailed measurements of the environment for an entire perihelion passage.

In principle, the interaction of the two flows (cometary and solar wind) can be described by the idea of a **mass-loaded plasma**. The addition of the slow, heavy cometary ions to the high velocity solar wind leads to the modification of both the cometary and solar wind plasmas. The degree to which the solar wind is mass-loaded depends on the number of cometary ions produced per second, which in turn depends on the outgassing rate of the cometary neutrals. Both are mostly anti-correlated with the heliocentric distance of the comet, although there are also small-scale variations depending on other parameters.

A magnetohydrodynamic approach (multi- or single-fluid) for the mass-loaded plasma can approximate the interaction region, but leaves many effects at scales smaller than the ion gyroradius unsolved. At comets, the ion gyroradius is often much larger than typical length scales, this was explored by e.g. [93] in Hybrid simulations,

results of which are shown in Fig. 1. In some instances, even electron scales need to be taken into account to understand large-scale features [28].

Ordered by the neutral outgassing rate  $Q$ , the interaction generally falls into one of three regimes, which are illustrated in Fig. 2.

**The strongly active comet:**  $Q > 5 \times 10^{27} \text{s}^{-1}$  This is the classical comet plasma picture as it was known from the missions to comets 1P, 19P/Borelly, 21P, and 26P/Grigg-Skjellerup (26P). Boundaries like the bow shock and diamagnetic cavity have formed [113]. The inner coma is closer to photo-chemical equilibrium and collisions between ions and neutrals are important. A plasma tail is visible. There are waves far upstream of the bow shock from the pickup of cometary ions [22].

**The intermediately active comet:**  $5 \times 10^{26} \text{s}^{-1} < Q < 5 \times 10^{27} \text{s}^{-1}$  At this stage, the solar wind is deflected and decelerated significantly, as a result of the presence of cometary ions. First boundaries form, but can disappear and reform on short timescales [65]. The interplanetary magnetic field starts to drape around the obstacle ion cloud.

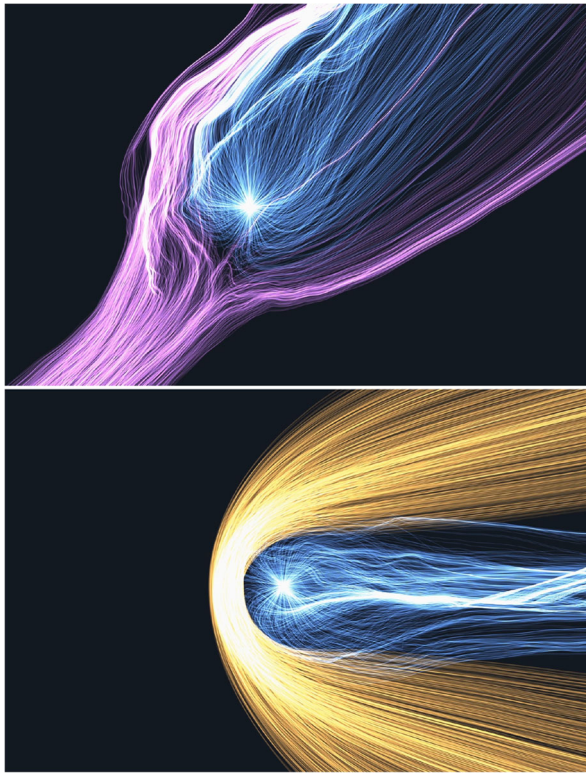


**Fig. 1** Simulations of cometary plasma. Top: stream lines of solar wind and cometary ions. Bottom: magnetic field lines and cometary ion stream lines (Technische Universität Braunschweig and Deutsches Zentrum für Luft- und Raumfahrt; Visualisation: Zuse-Institut Berlin)

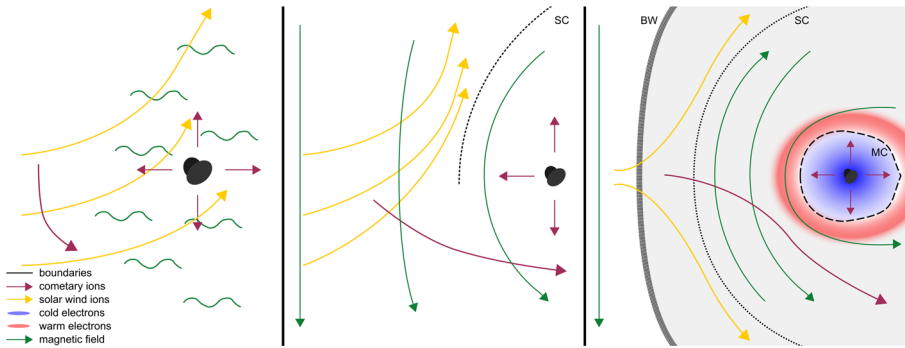


**Fig. 2** A sketch of the cometary plasma environment in the plane containing the magnetic field and the solar wind flow. The three panels show different stages, left: weak activity, middle: intermediate activity, right: high activity. Boundaries and regions are labelled: bow wave (BW), solar wind ion cavity (SC), and diamagnetic cavity (MC). Adapted from [62]

**The weakly active comet:**  $Q < 5 \times 10^{26} \text{ s}^{-1}$  No boundaries have formed yet. The influence of cometary ions on the solar wind is small. The magnetic field is usually only slightly elevated compared to solar wind values [60] and the plasma density follows a typical  $1/r$  profile that is modulated by the neutral outgassing rate [34, 48]. There are ultra-low frequency waves detected in the magnetic field and plasma density [18, 126].

A comet, along its journey around the Sun, may move to higher outgassing regimes while others remain weakly active throughout. Comet 67P went through all three stages listed above during the Rosetta mission [73].

## 2 A review of large scale structures in the interaction region

### 2.1 Bow shock

**The bow shock has been observed at several active comets** and has been modelled extensively [93]. Figure 2 shows schematic images of solar wind interaction with a comet, and the bow shock appears in the right-hand panel. The bow shock moves outwards as the mass-loading increases, and can be millions of km from the nucleus in comets with high gas production rates, whereas at low gas production rates (e.g. 26P) the critical point for shock formation is never reached and no bow shock forms; instead a more gradual increase in magnetic field (a bow wave) is observed [132]. At comet Halley, the bow shock was observed by Giotto only on the inbound pass, and a bow wave could be observed outbound. At comet 67P, the trajectory of the Rosetta spacecraft did not allow for an in situ observation of a bow shock or bow wave, but a structure in the plasma environment at lower gas production rates was identified as an infant bow shock, a highly asymmetric structure that behaves like a shock and is confined to one hemisphere of the interaction region, as illustrated in the middle panel of Fig. 2 [65].

**Bow shocks are not unique to the comet plasma environment**, and they have also been seen at all planets. At Mars, the bow shock is largely symmetric, and its mean location is steady and only weakly affected by solar cycle variations [105]. For both Mars and Venus, the position of the bow shock has been found to be more influenced by solar Extreme UltraViolet (EUV) radiation than by solar wind dynamic pressure [72, 135].

The bow shock at a comet reacts to increased ionisation rates in the same way as the bow shocks at Mars and Venus. It has been shown in simulations that the standoff distance of a cometary bow shock increases with an increasing ionisation rate. The more realistic simulations are made by including additional ionisation processes — photo-ionisation, electron–impact ionisation, and charge exchange — the farther upstream from the nucleus the bow shock moves [137]. The acceleration of newly created pickup ions differs on the upstream and downstream sides of the shock. Therefore a pickup ion energy spectrum can be used to estimate the standoff distance of a bow shock, as was shown in simulations [3] and this was used to estimate the position of the bow shock at comet 67P when the spacecraft was located far downstream [119].

A multitude of upstream wave phenomena have been observed at both Mars, Earth, and Venus (e.g. [30, 91, 105]). Waves were also observed in the foreshock of comet 1P [122], and future detailed observations in the upstream region of a cometary bow shock would be expected to show similar features. This would include back-scattered particles that contribute to wave growth, which has been seen at all three of the terrestrial planets.

## 2.2 Solar wind ion cavity

When comet 67P was about 1.8 AU from the Sun, solar wind ions could no longer reach the inner coma [118], observable as a lack of solar wind ions in the in-situ observations (see Fig. 3). The **region that is devoid of solar wind ions** is called the solar wind ion cavity [9, 138]. Closely upstream of the solar wind ion cavity, **solar wind ions are seen to be significantly deflected** from their original anti-sunward motion, and protons back-scattered toward the Sun have also been detected [9]. The location of this region changes with gas production rate and upstream solar wind

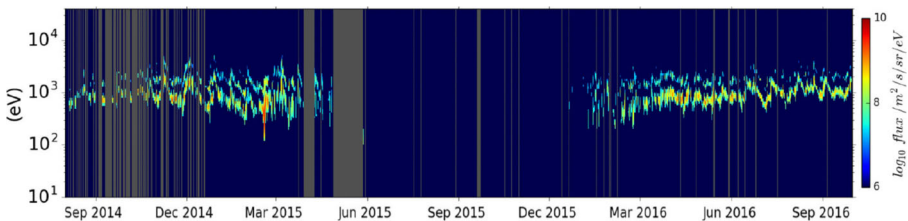


**Fig. 3** Energy spectrogram of the solar wind ions summed over all viewing directions and integrated over 1 hour for the entire Rosetta comet phase. One can see clearly that the spacecraft was located in a solar wind ion free region during the months around comet 67P perihelion (August 2015), when the gas production rate was highest. Adapted from [118]

parameters. For example, it was observed at comet 67P, that an interplanetary coronal mass ejection (ICME) could push solar wind ions closer to the inner coma, so that Rosetta, previously in the solar wind ion cavity, could observe protons for a short period of time [35]. A region from which the solar wind was excluded was also seen at comet 26P [87], and at comet Halley. The boundary that separates the solar wind ions from the solar wind ion cavity at comet 1P has been given many different names in the literature depending on what aspect of it was under study. For example the term *cometopause* has been used both to describe where cometary ions dominate over solar wind ions [50] and to mean a solar wind charge-exchange collisionopause [25], i. e. a boundary where charge-exchange collisions first become important. A similar boundary has been called the Induced Magnetosphere Boundary at Mars [100] and Venus [158]. More than one physical mechanism is likely to be involved in its formation, as both collisional effects, magnetic pileup, and ion chemistry are important in this region. See [22] for a review of the many aspects relevant to this boundary at comets.

### 2.3 Diamagnetic cavity

Early on in cometary plasma physics, [15] and [49] realised that one consequence of mass-loading is the deceleration of the incoming (solar wind) flow. The ultimate consequence of this is that the flow comes to a halt at some cometocentric distance  $r_c$  if mass-loading is sufficient. Although the magnetic field was not part of their simple fluid models, they realised that as long as the magnetic field was frozen into the flow, it would also stop at this distance. As comet nuclei are not magnetised [5], it was speculated that a field-free diamagnetic cavity would form. However, this region can only be sustained if the magnetic field diffusion into it is prevented. Early on it was speculated that simply the dynamic pressure of the outflowing cometary ions would be sufficient to balance the magnetic pressure and prevent diffusion into the cavity.

In preparation for the space missions to comet 1P/Halley, an **artificial comet experiment** (AMPTE, [146]) was designed and launched. The main goal was to investigate the interaction of the solar wind and magnetospheric plasma with a cloud of heavy ions, in this case Barium or Lithium. The plasma parameters of these experiments were very similar to the parameters during the 1P flybys.

In regards to the formation mechanism of the diamagnetic cavity at the artificial comet, two models have been presented: [69] showed that the dynamic pressure of the expanding ion cloud is sufficient to stave off the magnetic field, whereas [146] and [99] showed that the thermal pressure of the electrons could also be responsible. [130] showed that in numerical simulations, the dynamic pressure was the more favourable of the two mechanisms. No other studies were conducted and so far, none of the two mechanisms could be ruled out entirely.

With the 1P flyby of ESA's Giotto spacecraft, new light was shed on the **diamagnetic cavity shape and formation mechanism**. It was quickly found that neither the thermal pressure nor the dynamic pressure would be sufficient to uphold the diamagnetic cavity, because neither of them showed a significant change at the boundary [23]. So [23, 24] presented an alternative mechanism: the **ion–neutral friction force**. For this mechanism it was assumed that the magnetic field in the upstream region

had already reached a stagnation point and the charge-exchange collisions between the outward streaming neutrals and the ions at rest could balance the magnetic field pressure. This of course assumes that the ion–neutral coupling is efficient, which was consistent with observations of the ion and neutral speeds being very similar. [24] derived a magnetic field profile in the boundary region and a standoff distance for the diamagnetic cavity that fit well with the observations by the Giotto magnetometer.

[112] then pointed out that the diamagnetic cavity boundary was very likely not spherical in shape, as the boundary normal was a better fit to an unstable boundary. Indeed, [41] and [40] found that the boundary might be unstable to the Flute and Kelvin-Helmholtz instabilities. This was later confirmed in simulations by [129], who found that the boundary was rippled. However, no measurements had yet confirmed this.

With the arrival of the Rosetta spacecraft at comet 67P, the diamagnetic cavity could be investigated in more detail [59]. Rosetta entered the cavity over 700 times, although it should be noted that because of the negligible speed of the spacecraft this means that the boundary was moving over the spacecraft and not the other way around as was the case of Giotto at 1P. Figure 4 shows example magnetic field measurements at both comets.

[58] and [62] reported that the diamagnetic cavity size was strongly correlated to the local outgassing rate (derived from in situ measurements of the neutral gas density). As expected, the diamagnetic cavity expands with increasing outgassing rate. It was also found that the boundary normal was inconsistent with a spherical shape, indicating again that the boundary was rippled and highly unstable.

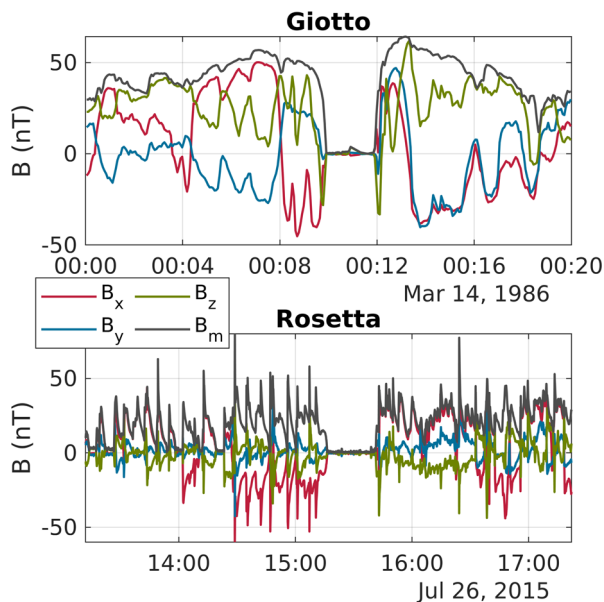


**Fig. 4** Magnetic field observations of cavities at 1P (measured by Giotto's magnetometer) and 67P (measured by the magnetometer onboard Rosetta)



However, it was found that **the ion–neutral friction force was not the driving parameter** behind the cavity formation at comet 67P, as the measurements of the ion velocity indicated that the coupling of ions and neutrals was inefficient due to lower neutral densities at 67P compared to 1P [121, 151]. Additionally, the ion density profile that was assumed for comet 1P was not applicable at 67P, due to transport of the ions being as important as recombination [12]. However, [76] found that the electron exobase was a good ordering parameter for the diamagnetic cavity detections, indicating the importance of electron–neutral interactions in this regime. As of now the formation mechanism of the diamagnetic cavity at 67P is still unknown.

## 2.4 Plasma tail

Comets can have more than one tail: in addition to the most clearly visible dust tail there is an ion or plasma tail shown in remote observations like the one illustrated in Fig. 5. While the dust grains in the dust tail are pushed away from the Sun by the photon pressure, the sunlight cannot explain the formation of a plasma tail. This led [14] to propose the **existence of a solar wind**, and [2] to develop a theory for how the solar wind magnetic field lines are draped around the comet. Alfvén’s theory was supported by observations at comet 21P by [141], who observed that “The structure

**Fig. 5** Photograph of Comet Morehouse, [125]





of the 21P magnetotail was quite similar in many respects to that observed at Venus.” Plasma tails can have an enormous length of over 3 AU, as evidenced by some of Ulysses’ fortuitous comet tail crossings [57, 88]. Tangential discontinuities in the solar wind approaching a comet, as seen in the magnetic field measurements in the coma of comet 1P/Halley [128], can lead to a more complicated magnetic structure characterised by “nested draping” in the plasma tail.

Rays of light pointing away from the nucleus over a range of directions are often seen in telescope images of comets [124] and it has been suggested that the formation of such cometary rays is related to ionisation processes in the coma [125]. To date there are no in situ observations of cometary rays.

Remote observations sometimes show that the tail pattern is disrupted and **the tail appears broken or disconnected**. Usually a new tail forms quite quickly [152]. Three different categories of triggers have been proposed: a shock wave, a magnetic field reversal and a high solar wind dynamic pressure event.

**Shock wave** [154] proposed that a shock wave travelling down the tail would rarefy and compress the plasma in the tail, which appears to a remote observer as a succession of regions with and without cometary plasma. Thus, in this model, a tail disconnection event is not a real disconnection, it just appears as one to a remote observer.

**Magnetic field reversal** [116] proposed that a field reversal at a discontinuity in the solar wind, like an interplanetary coronal mass ejection, could also trigger reconnection when the discontinuity hits the coma and that this could lead to a disconnection event. Although the reconnection region would be on the dayside, the disturbed plasma may travel towards the tail and cause a real disconnection of the field lines from the inner coma. This would only be possible at very active comets, where the pile-up of the magnetic field is sufficient.

**High solar wind dynamic pressure** [83] proposed that a flute instability that is triggered in the cometsphere due to higher solar wind dynamic pressure could propagate into the tail and develop into an apparent tail disconnection.

Because tail disconnections occur in the far tail, in situ observations are difficult to do. Although some far tails have been crossed (e.g. [115]) these observations have been too short to investigate disconnection events. Thus, there have not been any in situ observations of a tail disconnection, and the cause of tail disconnections remains an open question.

### 3 A review of plasma processes at a comet

#### 3.1 Collisions in the coma

**Solar wind ion interaction with the neutral coma** In a charge exchange reaction, one or several electrons are semi-resonantly transferred between a neutral particle

(atom or molecule) and an ion. Such ion-neutral reactions between incoming, usually fast, ions and a correspondingly slow-moving neutral environment are ubiquitously present in astrophysics environments [31, 153]. Renewed interest in these reactions was kick-started by the discovery that comets are soft X-ray emitters [98], due to highly-charged solar wind ions charge-exchanging with the neutral coma [26].

As illustrated in Fig. 6, single charge-exchange reactions between, for instance, solar wind protons and the neutral gas M take the form  $H^+ + M \rightarrow H + M^+$ : from the point of view of the ions, the net effect is to **replace a fast, light ion (solar wind ion) with a slow heavy one (newly-born cometary ion)**. Energetic neutral atoms of hydrogen can be a by-product of the reaction (see, e.g. [117]). Because the cometary neutral coma is in radial expansion from the nucleus, charge-exchange reactions act cumulatively over distances of hundreds of thousands of kilometres upstream of the nucleus, hence critically contributing to the mass-loading of the plasma, its large-scale dynamics, and to the formation of typical structures such as the bow shock [61, 137, 140].

Slowing-down of solar wind ions due to mass-loading and heating around the shock-like structure ahead of the nucleus are expected, which may call for the use of **energy-dependent cross sections** depending on the severity of these effects [138–140]. The gas production rate of a comet can be estimated, using a model of charge exchange in the coma and in situ flux measurements of the charge state distribution of solar wind ions [136, 138–140]. This may even lead to measurable X-ray emissions [68].

**Cometary plasma interaction with the neutral coma** Photo-electrons, produced by solar EUV radiation ionising the neutral coma, are born with energies typically

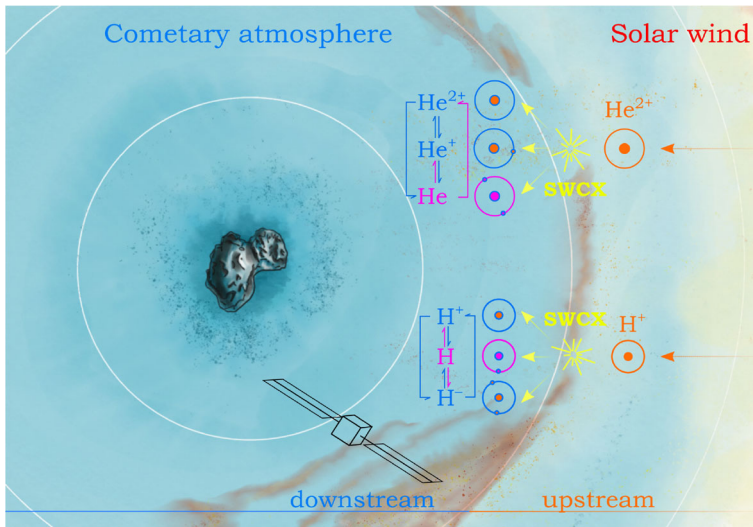


**Fig. 6** Solar wind charge-exchange interactions at comet 67P [139]

around 10 eV. At comet 67P, a supra-thermal electron population was found, peaking in the 30–40 eV energy range [19]. These electrons, in turn, produce secondary electrons below  $\sim 12$  eV. This picture has been confirmed by plasma measurements, which showed that the bulk of the electron population at comet 67P was warm (5–10 eV) at heliocentric distances above 3 AU [38, 39, 52].

When comet 67P was at heliocentric distances between 3 AU and perihelion (1.24 AU), there was, in addition to the warm component, a **cold electron population** with temperatures below 1 eV [38]. This cold population is a result of electron cooling through collisions with the neutral gas [39, 121]. For very high outgassing conditions, for example comet 1P at 0.9 AU, cold electrons have been predicted to be dominant in the inner coma [51].

At comet 67P it was found that, while electron impact ionisation dominates plasma production at large heliocentric distances and during transient solar wind events [71], photo-ionisation is the main source of the plasma near perihelion [80]. There, the coma starts to be optically thick to solar EUV radiation due to absorption by the neutral coma [12] and the dust [84]. Transport was found to be the dominant loss process at comet 67P throughout the Rosetta mission, and dissociative recombination could be significant only close to perihelion [12].

Modelling the cometary plasma density, taking both sources and losses into account, showed excellent agreement with Rosetta multi-instrument observations [48, 80] at large heliocentric distances ( $> 3$  AU), all the way down to the surface [78]. In these models, the ions were assumed to move at the same speed as the neutrals. Therefore, the agreement with data implies that no significant ion acceleration took place within about 70 km from the nucleus. For comet 67P close to perihelion, such models overestimate the plasma density, which indicates that a significant ion acceleration took place in agreement with observations by [121]. A presence of nanograins may also have influenced the electron density [84].

For very high outgassing conditions, for example comet 1P at 0.9 AU, the plasma can be assumed to be in photo-chemical equilibrium and ion–electron dissociative recombination would be the dominating loss process [24].

Ion–neutral collisions are significant in determining **the composition of the plasma**. Charge-changing collisions (an umbrella term that also encompasses charge-exchange reactions [140]), which may transfer an electron (e.g.,  $\text{H}_2\text{O}^+ + \text{CO}_2 \rightarrow \text{H}_2\text{O} + \text{CO}_2^+$ ) or a proton (e.g.,  $\text{H}_2\text{O}^+ + \text{H}_2\text{O} \rightarrow \text{H}_3\text{O}^+ + \text{HO}$ ) between ions and neutrals, have an influence on both the mass and velocity distributions of the ions. They therefore play a role in mass loading [143]. Several ion species were found for low outgassing conditions at comet 67P [44]. While some of these, like  $\text{H}_2\text{O}^+$  and  $\text{O}^+$ , can be produced directly through ionisation, others, like  $\text{H}_3\text{O}^+$ , only result from ion–neutral chemistry. Their presence shows that the coma was not fully collisionless. Near perihelion the  $\text{H}_3\text{O}^+$  to  $\text{H}_2\text{O}^+$  ratio was found to be highly variable [45], and neutral outgassing and ion–neutral collision frequency increased, favouring the production of new ions [77], in particular those produced by protonation of molecules with higher proton-affinity than that of water [149], for instance transforming  $\text{H}_2\text{O}^+$  to  $\text{NH}_4^+$  in the presence of  $\text{NH}_3$  [11]. Changes in the solar wind upstream conditions can change the composition of the neutral coma even on short time scales [120].

### 3.2 Electric fields

The three most important contributions to the DC electric field in the inner coma are the solar wind **convectonal** electric field, the **ambipolar** field, and the **polarisation** electric field.

In the inner coma, the electrons are hotter than the ions and can escape much faster radially outward from the nucleus. This creates an **ambipolar** electric field (directed radially outward) that accelerates the ions and slows down the outward motion of the electrons. [148] have shown that the presence of an electric field can dominate over the effects of collisions and result in much higher ion velocities than predicted based on measurements at 1P. This was confirmed by Langmuir probe measurements in and near the diamagnetic cavity of comet 67P [121]. Also for low outgassing conditions, the ion motion can be faster than the neutral motion as a result of convective and ambipolar fields acting on the ions [10, 94]. However, this is only the case for larger cometocentric distances, close to the nucleus ( $< 10$  km) no acceleration could be observed [78].

In the inner coma of a weakly outgassing comet, the ions are unmagnetised and therefore, water group ions, newly created by ionisation, move in the direction of the electric field. Electrons, on the other hand, are magnetised and their motion is governed by an  $\vec{E} \times \vec{B}$  drift perpendicular to both the magnetic and electric fields. This leads to a charge separation, which in turn gives rise to a polarisation electric field [119]. Particle-in-cell simulations including all three field contributions have confirmed the existence of a polarisation field in agreement with Rosetta observations [67], and implicit particle in cell simulations have been seen to produce similar results [29].

For highly active comets and on large scales, where an MHD description is adequate, the difference in electron and ion motion may be described by a Hall electric field [82].

### 3.3 Magnetic field carriers

The heavy ions in the cometary plasma are not magnetised, whereas the electrons are. Additionally, it has been shown that electron-scale physics are important even on larger scales [28].

The solar wind ion cavity is purely a region devoid of solar wind ions, not of solar wind electrons and not of the solar wind magnetic field. Thus, understanding **the flow of the electron fluid** is instrumental in understanding the behaviour of the magnetic field.

**The particle signatures at the diamagnetic cavity** are of particular interest. Cold electrons are present in the diamagnetic cavity and to a lesser degree outside of it [121]. It has been observed that a suprathermal electron population associated with the solar wind is present just outside the cavity, but not inside [101, 111]. Consequently, as the solar wind flow is mass-loaded the protons decouple from the field first, forming the solar wind ion cavity. Then at the diamagnetic cavity boundary, the magnetic field is stopped and so are the associated electrons.

### 3.4 Waves

Plasma waves take on an important role in the cometary plasma environment, **transferring energy** across boundaries and **heating particle populations** through wave–particle interactions. Waves are also instrumental in **setting up plasma boundaries** around the comet, e.g. the bow shock is formed when the relative velocity between the solar wind and the cometary plasma exceeds the wave speed [21].

A wide variety of plasma waves were detected starting millions of kilometres from the nucleus down to the closest approach at approximately 8000 km for the ICE spacecraft at 21P and the VEGA-2 spacecraft at Halley [131, 144]. **Ion acoustic waves** were detected by the ICE spacecraft during its traversal of the bow shock region at 21P [132], and by the Sakigake spacecraft in the foreshock region upstream of Halley's comet [122]. The Rosetta spacecraft observed ion acoustic waves both before the formation of the diamagnetic cavity [64] and later, when the cavity had formed, such waves were seen to be confined inside the cavity [63]. In the plasma outside of the diamagnetic cavity, wave activity in the **lower hybrid frequency range** is abundant [4, 89], and waves in this frequency range have also been observed at the boundary of the diamagnetic cavity [102], indicating that a **mode conversion** from lower hybrid to ion acoustic waves takes place at the boundary. One of the first discoveries by the Rosetta spacecraft was the **“singing comet” waves** that were found at low frequencies [126, about 40 mHz; 127]. These waves have been shown to be compressional [18], and they have been interpreted as the result of a modified ion-Weibel instability [107].

**Mirror mode** structures were observed in the magnetosheath of comet 21P [145] and on both sides of the magnetic pileup boundary of comet 1P/Halley [55]. **Ion cyclotron waves** at the gyro frequency of water group ions were observed at comets 21P [142], 1P/Halley [53, 157] and 26P [54, 114]. While both ion cyclotron and mirror mode waves were prominent during these comet encounters, they have, so far, eluded detection by the Rosetta spacecraft at its comet.

Thus, a wide variety of waves were observed in the fast flybys in the 1980s and 90s; recently the Rosetta mission has continued to find new plasma wave modes, and the waves have been seen to be linked to boundaries such as the bow shock and the diamagnetic cavity boundary. Still there are differences between the comets, and these are largely unexplained at this time.

### 3.5 Energetic neutral atoms

Energetic neutral atoms (ENA) are created when an energetic ion undergoes a **charge-exchange reaction** with a neutral atom or molecule, creating an energetic neutral atom (or molecule). **Charge exchange processes may remove much of the charge of the solar wind at a comet**, producing a neutral solar wind that may strike the inner collisional coma or the nucleus [117, 136]. Charge exchange reactions with the solar wind are sometimes a significant source of ionisation of the coma [137].

Charge exchange between cometary ions and neutrals is the most important collisional process in the marginally collisional coma, acting to slow down the ions while creating a component of low energy ENAs [148].

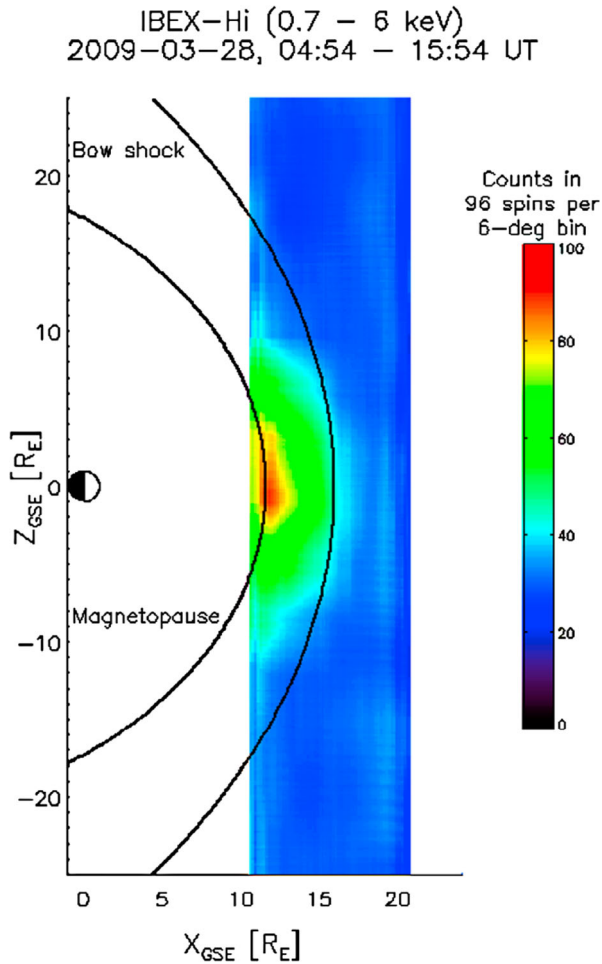


**Fig. 7** ENA emissions from the subsolar magnetopause of Earth [43]

No ENA instrument has been flown to a comet yet. [36] conducted MHD simulations of a comet and found that remote observations at large distances should be feasible. **A comet shines bright in ENAs.** Charge exchange products can also be seen by ion instruments in the form of  $\text{He}^+$  ions produced from solar wind  $\text{He}^{2+}$  [136, 138, 139]. These observations can be used to independently assess the integrated **column density of the neutral atmosphere upstream** of the observation point [73, 136].

Other missions have measured ENA emissions from objects that are similar to comets. For example, the Interstellar Boundary Explorer (IBEX) observed ENAs produced at the outer boundary of the heliosphere, the heliopause region [106], which has many similarities to the situation at a comet on a much grander scale. Two plasma streams meet (the solar wind and the ionised part of the interstellar medium) in a

region with a significant neutral gas background. IBEX has also been used to obtain an overall image of the plasma structures of the Earth's magnetosphere (see Fig. 7 and [43]). Another example relevant to comet studies are the observations of the sub-solar magnetopause ENA jet at Mars. This jet is affected by the solar wind pressure, and that raises the possibility of a continuous remote monitoring of the effect of the solar wind on a magnetosphere [46]. The ENA jet at Mars showed a periodic oscillation after the impact of an interplanetary shock passage, indicating that an oscillation of the boundary was excited [47].

### 3.6 Influence on the nucleus

The solar wind can directly influence the nucleus by solar wind ions hitting the surface, if the comet atmosphere is not too dense. **Solar wind sputtering of the surface** can release elements like Na, K, Si, and Ca, which are less volatile than the typically released compounds  $\text{H}_2\text{O}$ , CO, and  $\text{CO}_2$ . These less volatile materials were detected by ROSINA on Rosetta [155], and were seen released from different areas of the nucleus than the volatile species. This could be due to the deflected solar wind hitting different parts of the nucleus than the sunlight or the lower degrees of attenuation of solar wind protons above the hemisphere of lower activity where the sputtered species have been observed. The release of surface materials by sputtering can be calculated through models [159], and thus the chemical composition of major elements of the areas affected by sputtering inferred from gas composition measurements [133].

Sputtering often releases metals, which are ionised quickly and recombine slowly. They may therefore form long-lived metal ions, like the sporadic E layers observed in the ionosphere of Earth [92].

Energetic molecules hitting the surface may also participate in **surface reactions**, thus affecting the chemistry at the nucleus. [156] for example suggested that Eley-Rideal reactions could be the source of  $\text{O}_2$  detected at comet 67P. [79] later showed that this was not a plausible explanation at comet 67P, but it could still be a relevant mechanism for formation of other molecules. Sputtering is in general important for icy surfaces, not only at comets but also at icy moons [86].

## 4 A review of dust–plasma interactions

None of the instruments on previous comet missions were well suited to investigate how the plasma and dust interact, so many open questions remain. The cometary environment is a region where physics of dusty plasmas is important and accessible to in situ study by visiting spacecraft [108, 150]. Studying the dusty plasma at comets is also relevant to other bodies, e. g. at Enceladus [16]. There, Cassini observations indicate that only a small fraction of the electrons escape attachment to dust grains and the dust consequently is of major importance for the plasma dynamics [37, 110].

However, the **dust size distributions** in the two environments differ significantly, and so does the relative importance of dust-plasma interactions. Describing this distribution as a power law, the spectral index is approximately 4–5 at Enceladus and in the E-ring [90, 95]. At 67P, Rosetta found a less steep dust distribution, with a spectral



index  $\sim 3$  for grain masses below 1 mg (corresponding to mm size), increasing to 3.6 post-perihelion [42]. Thus, for the same dust mass in a unit volume of space, fewer electrons attach to the dust grains as many small grains have much higher total capacitance than one large grain of the same mass and the voltage they can charge to is limited by the kinetic energy of electrons in the plasma, and therefore the dust-plasma interaction is weaker [37]. There are few Rosetta observations of dust grains below  $\mu\text{m}$  size, and subunits of larger grains have been found down to about  $0.1 \mu\text{m}$  [103].

A number of different processes can lead to the fragmentation of particles and in contexts with Rosetta results, the fragmentation due to electric surface charge of the dust grains was in particular discussed [81]. Thus, not only does the size distribution influence the grain charge as described above, but **there is also an influence of the grain charge on the size distribution through fragmentation of dust grains**. As a result, if the plasma is well characterised and the charging processes are known, the dust size distribution will provide **information about the cohesive strength of the grains**.

Charged dust grains in the sub-micrometre size range are moved by electromagnetic forces and, in regions where the gas density is high, also by the drag force from the neutral gas. Charged nano-grains were detected by the electron spectrometer onboard the Rosetta spacecraft [20]. Due to the small charge-to-mass ratio, charged nano-dust trajectories have a large radius of curvature, and they are approximately parallel to the electric field. Rosetta results have shown that the electric field around a comet is highly structured (Section 3.2), which affects the motion of the charged dust. For example, the ambipolar electric field would act to confine negatively charged grains to the inner coma. The interaction also goes the other way: the collection of electrons on the much heavier dust grains affects how the electric field is structured in the coma, and the presence of dust influences the wave modes in the plasma, such as dust acoustic and dust ion acoustic waves [8, 109]. Figure 8 shows dust acoustic waves in the laboratory as an example of dust-plasma interactions.

## 5 Future science questions

### 5.1 Large scale structures in the interaction region

#### 5.1.1 Bow shock

Simulations have shown that the location of the bow shock is asymmetric along the direction of the solar wind convective electric field [93] to a greater extent than what has been seen at Mars [105], and this asymmetry is highly dependent on cometary activity and solar EUV intensity [97]. Not all flybys of comets show a well defined shock, sometimes only a bow wave was observed [114]. It was not possible to observe a fully developed bow shock with Rosetta, due to spacecraft trajectory constraints. This also means that the shape of a cometary bow shock has never been observed. At planets, data from different locations, probed during many spacecraft orbits, has been used to form a statistical picture of a mean bow shock shape. While a snapshot of the bow shock shape at one moment in time would require multi-point measurements,

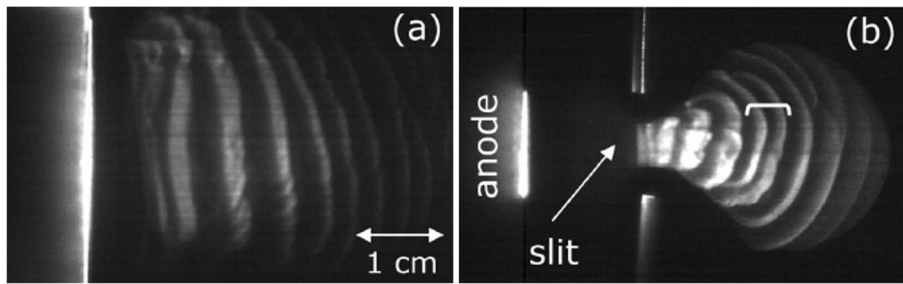


**Fig. 8** Dust acoustic waves [75]

single-point observations can be used to determine what the bow shock shape is on average if the data set covers a sufficiently large range of positions. At comets, all we have so far are single point measurements in flybys and Rosetta observations from a small region over which an infant bow shock moved at different times [65]. Therefore, the bow shock shape, width, and structure have not been adequately determined and are largely unknown.

In modelling, the shape of a bow shock and its width are direct consequences of the assumptions on which the models are based. Verifying the shape observationally is therefore important for our understanding of the physics governing the formation of bow shocks at comets. This is particularly true in the case of a bow shock under formation, that is to say, an infant bow shock, which cannot be studied at Solar System objects of any other kind. Therefore the main question is

### ⇒ **How asymmetric are large-scale structures at comets?**

The infant bow shock as it was observed was not always constant, instead changes could be seen on varying timescales [65]. What is driving these changes? Are they driven by changes in the upstream solar wind, by variable outgassing from the nucleus or is the bow shock itself unstable, leading to waves that are seen as variable conditions by a stationary observer? At Earth bow shock ripples have been observed in multi-spacecraft studies [85]. Bow shock ripples are thought to be a cause of high-speed jets (or plasmoids) in Earth's magnetosheath, and such jets have been found to be capable of causing a geomagnetic disturbance [123]. Do cometary bow shocks support surface waves and ripples? Can ripples lead to jet formation at comets, and if so what would the impact of those jets be on the plasma and coma downstream of the shock? How do these bow shock properties develop as the bow shock transforms from an infant to a fully developed shock? The answers to these questions will have an impact on our understanding not only of cometary bow shocks, but also of both the comet–solar wind system as a whole and of the physics of bow shocks in general.

What heats the plasma as it passes the shock? Is it heated by reflection followed by thermalisation or by waves excited by plasma instabilities? Both these scenarios are known to occur at Earth [6, 33]. At a comet the situation is more complicated than at a planet, since in the vicinity of a cometary bow shock there are both cometary ions and neutrals present. Additional phenomena seen at Earth's bow shock that remain unexplored at comets include electric fields at the shock that may contribute to charged

particle reflection, acceleration, and heating; field-aligned particle beams; and fore-shock waves in a variety of frequency ranges. These questions form part of the more general problem of how mass, energy and momentum are transferred in the cometary environment, through the coma and across boundaries.

### 5.1.2 Solar wind ion cavity

It is known from both the Rosetta observations and previous in situ measurements, in fast flybys of comets, that once a comet is active enough a boundary which demarcates the region that solar wind ions cannot penetrate is formed. Other boundaries have been identified in this region of the plasma that could not be found in the Rosetta observations. Therefore, we ask:

⇒ **Which boundaries exist at a comet during its journey through the Solar System?**

Is the solar wind ion cavity the only boundary in the cometsheath? What causes the formation of this boundary? How important are different physical processes, such as mass-loading, magnetic pileup, ionisation processes, and the wide variety of collisional processes at work at a comet? These questions remain unanswered today, and answering them would require multi-point measurements to determine how the boundary is structured as well as quantitative observations of collisional processes in the coma. Additional information can be provided by ENA measurements, observing the main regions of a comet magnetosphere remotely. The relative importance of the mechanisms involved is likely to change during the course of a comet's orbit around the Sun. Thus, conducting multi-point measurements at a range of heliocentric distances, we can advance our ability to predict boundary properties under varying conditions. Such knowledge will be of significance to planetary studies, including exoplanets, since at unmagnetised planets a corresponding boundary, the induced magnetosphere boundary, is responsible for protection from atmospheric escape [66].

### 5.1.3 Diamagnetic cavity

The main open question that remains with regards to the diamagnetic cavity is

⇒ **What are the processes behind the diamagnetic cavity formation? Is it different for 67P and 1P?**

The mechanism of cavity formation is still poorly understood, with theories diverging for the two comets at which this region has been observed.

Unfortunately, Rosetta was not able to measure the distribution function of the lower energy ions [104] due to a very negative spacecraft potential. These ions are instrumental in understanding the plasma dynamics at the boundary as their direction and speed can give insight into the particle dynamics at the boundary and their interaction with the neutral gas. This in turn will provide more information on the diamagnetic cavity formation mechanism.

The distribution function of the electrons is also poorly understood. The interplay of newly created warm photo-electrons, cold electrons, and suprathermal electrons

has not been investigated in detail and available data are severely lacking in accuracy and temporal resolution. New observations with higher temporal resolution, better angular coverage, and at low spacecraft potential are needed to understand these dynamics.

Furthermore, the true shape of the boundary has not been measured, as this requires measurements at at least two points of the boundary at the same time. It remains to be investigated with the help of multi-point measurements what the exact nature of the boundary oscillations is. It is unclear how these oscillations are affected by a change in the gas production rate. Are the oscillations large and fast enough to explain the quick succession of diamagnetic cavity encounters at 67P?

The situation at both Mars and Venus should be very similar to the one at the comet, but no observations of a completely field free region have been reported there. However, it should be noted that the distance at which this boundary might be detected is most of the time below the spacecraft trajectories.

#### **5.1.4 Plasma tail**

Tail disconnections have been revealed by remote optical observations, and tail rays can also be seen in pictures of comets. In the absence of comprehensive in situ measurements from comet tails, all that exist are a few fast fly-throughs, the mechanisms behind these phenomena are as yet unknown.

##### **⇒ What is the cause of tail disconnection events and tail rays?**

Various theories have been proposed to explain tail disconnection events (see Section 2.4), but none of these give a complete and satisfactory answer. Answering this question will, in turn, teach us a great deal about the cometary plasma environment. Is reconnection a relevant concept in comet plasma physics? What causes ionisation and plasma acceleration in comet rays? And why are there rays at all, as opposed to a uniform expansion in all directions? Furthermore, observing the comet tail plasma in situ will reveal how the tail is structured, what plasma instabilities are present, and how this compares to the plasma tails of unmagnetised planets.

#### **5.2 Plasma processes at a comet**

##### **5.2.1 Collisions in the coma**

A comet presents an excellent opportunity to monitor the collisionality and evolution of a partially ionised environment. Due to the elliptical orbits of comets, the ion coma evolves and transitions between the collisional and collisionless regimes. This will help us understand how collisions compete with other processes on the microscopic level and how these effects influence a large scale system, that is to say, the comet as a whole.

##### **⇒ What is the role of collisions in the densest part of the coma?**

Despite past and recent sustained experimental efforts, many relevant cross sections for charge-changing and ionisation collisions, involving water or other abundant

species such as CO and CO<sub>2</sub> at energies below 1 keV, are not known with an accuracy sufficient to support accurate modelling of solar wind–cometary interaction. Also, the precise energy distribution of cross sections can play an important role when convolved with a heated solar wind ion distribution. Therefore, new extended laboratory experiments are needed to better constrain these cross sections and their shape at relevant energies. In turn, the investigation of the plasma composition at a comet can help constrain cross sections that are not accessible in the laboratory.

At low outgassing activity conditions ( $Q < 5 \times 10^{26} \text{ s}^{-1}$ ) cold electrons were observed at 67P [38, 52]. However, radial energy degradation models cannot explain the significant cooling of the newly-born electrons. The complex electromagnetic environment, as suggested by large scale simulations (e.g., [28]), may contribute to the energy budget of the cometary electrons.

At high outgassing activity conditions ( $Q > 5 \times 10^{27} \text{ s}^{-1}$ ), near perihelion at comet 67P, the diamagnetic cavity was observed near the electron exobase [76], where the electrons transition between the collisional and collisionless regimes. The formation mechanism of the diamagnetic cavity is a question in itself, and it is not known what role collisions may have in it.

For intermediate and high outgassing activity conditions ( $Q > 10^{27} \text{ s}^{-1}$ ), the ion composition changes and becomes richer as comets get closer to the Sun, which is evidence of ion–neutral collisions taking place [70, 77]. Rosetta observed hourly and daily variations of the triplet H<sub>2</sub>O<sup>+</sup>/H<sub>3</sub>O<sup>+</sup>/NH<sub>4</sub><sup>+</sup> at comet 67P, ruling out the idea of a steady-state ionosphere [11], but the reason behind the variability remains an open question.

A magnetised plasma streaming through a neutral background — like the solar wind streams through the coma — is the setting for the modified two-stream instability behind the “Critical Ionisation Velocity” hypothesis suggested by [1]. While kinetic energy is transferred from ions to electrons via a plasma instability, the actual ionisation happens in collisions between the energised electrons and the neutrals. The phenomenon has been observed in laboratory plasmas, but it has so far eluded detection in space [96].

We may formulate a number of specific science questions of importance on this topic; the following is a non-exhaustive list: (i) what is the role of charge-changing reactions in the local and large-scale dynamics (time scales, ion trajectories) of the plasma? (ii) how is energy transferred from the solar wind to the cometary plasma and neutral environment? (iii) how are the plasma boundaries formed at comets and what precise role do collisions play? (iv) how are electrons cooled in the inner coma? (v) why is the ion composition so variable? (vi) how stable is the ion–neutral two-stream interaction in a coma environment? and (vii) are negative ions abundant and what is their role? All these questions highlight the complicated interplay of collisional and electromagnetic processes in the cometary plasma.

Systematic investigation of charge-exchange effects with ion and ENA instruments concomitantly probing the cometary plasma, concentrating on the 3-D distribution of these species, will help shed light on these aspects. Moreover, the scope of all such studies far exceeds the sole dominion of comet–solar wind interactions – our understanding of planet–solar wind environments as well as that of other astrophysics environments (interstellar medium, etc.) will benefit from them.

### 5.2.2 Electric fields

The three major contributions to the DC electric fields at comet 67P have been identified following the Rosetta mission. At that comet, the DC fields were relatively more important than ion–neutral collisional coupling, in contrast to the results obtained at comet 1P. Thus, to understand the behaviour of the plasma, which is affected by the fields, we need to understand how the plasma interacts with the neutrals. In particular, detailed measurements of charged particle distributions around the comet will be necessary to enable us to understand how the fields are generated. The charged particle distributions are the source of the electric fields, and the fields affect the particle distributions. Thus, the formation of the electric fields is intimately linked to the effect of these same fields.

⇒ **How do electric fields contribute to energy, momentum, and mass transfer in the plasma?**

The formation of electric fields in the coma, as a result of interaction with the solar wind, affects the dynamics of both the cometary plasma and charged dust, transferring mass in the coma and tail. This, in turn, affects both tail properties and extended sources of gas released from the dust particles. Multi-point measurements of plasma, fields, and dust will elucidate the physics behind mass transfer and the consequences for both the coma and tail.

This topic is not limited to the large scale DC electric fields. Fields on small scales at the plasma boundaries, such as the bow shock and the diamagnetic cavity boundary, are likely to play a significant part in forming and maintaining these boundaries. Measuring these fields will advance our understanding of boundaries at comets.

### 5.2.3 Frozen-in condition and magnetic field carriers

In the solar wind, both electrons and ions are magnetised. In the diamagnetic cavity of a comet, neither ions nor electrons are. In between there is a region where the electrons are magnetised but the ions are not. The behaviour of the electrons at the interfaces between these regions is as yet unknown.

⇒ **What is the role of the electrons as magnetic field carriers in a plasma where the ions are not magnetised?**

The magnetic field is frozen-in to the electrons rather than the ions. There are regions with electrons of both solar wind and cometary origin and with several electron populations of different temperatures. If the various electron populations behave similarly with respect to the magnetic field, it is yet unclear to which electron population the magnetic field is frozen-in.

The problem of magnetisation is closely related to other questions about the plasma boundaries. What keeps the electrons outside the diamagnetic cavity from entering it? How is the current that maintains the difference in magnetic field intensity across the diamagnetic cavity boundary generated and maintained? What prevents the solar wind ions from entering the solar wind ion cavity, while allowing the solar wind electrons to pass through?

### 5.2.4 Waves

Previous space missions have found that waves are ubiquitous in the comet environment. However, it is not clear in which region of the coma these waves are present and how they depend on the activity level of the comet. Through multipoint measurements in the coma one can determine the temporal and spatial development of the waves. The details of wave propagation and the role of waves in diamagnetic boundary physics are not well understood. Going from single-spacecraft to multi-spacecraft observations will enable new insights into both the physics of the waves themselves and how they affect boundaries and the surrounding plasma. It has been speculated that wave–particle interaction and particle collisions transfer energy from the solar wind to the cometary plasma and redistribute energy in the coma.

#### ⇒ How do waves and wave–particle interactions affect the cometary plasma?

Wave measurements are a necessary part of the assessment of how energy is transferred in the cometary environment.

Waves on electron timescales, that is to say, near frequencies typical for electrons, such as the plasma frequency, are important as they influence the electron distribution function, and dissipate energy in the cometary plasma. At comet 67P, hot electron populations were observed outside the diamagnetic cavity, and at the infant bow shock. Capabilities to sample waves at the plasma frequency will enable measurements of this family of waves, and to further the understanding of energy conversion on electron scales.

Waves on ion time scales have been associated with the bow shock at comets 1P and 21P and with the diamagnetic cavity boundary at comet 67P. It has been proposed that the waves are driven by currents that flow at these boundaries. Therefore, wave measurements can aid the understanding of the boundaries themselves, and shine a light on both how plasma particles generate waves in the cometary plasma and how these waves contribute to heating of the particle populations.

The low frequency waves that have been observed: singing comet, mirror mode, and ion cyclotron waves are in principle understood in terms of plasma theory. However, the differences between the Rosetta observations at comet 67P and what was observed during the flybys of comets 1P, 21P, and 26P have not yet been completely explained. For example, why have no ion cyclotron waves been detected by Rosetta? The role of low frequency waves at comets, and how they are generated depending on cometary properties is an open question.

In dust–plasma relations, we know from observations that there is a distributed source of certain species [27, 32] and hence that there is a significant amount of dust in the coma. Charges bound to heavy dust particles give rise to new wave modes in the plasma [8, 109] and the detection of these waves provides an alternative measurement of the dust content.

### 5.2.5 Influence on the nucleus

That the nucleus affects the plasma in the coma is obvious, since outgassing from the nucleus is the source of the coma. However, the plasma can affect the surface of the



nucleus through sputtering and chemical reactions, thus changing the composition of the emitted gases. The plasma also has an influence on the charging of dust and of the surface of the nucleus itself.

### ⇒ **How do the plasma and the nucleus interact?**

How do particle fluxes to the nucleus affect the composition of the emitted gases? Whether detected gases have been embedded in the nucleus for billions of years or formed recently in surface–plasma interactions is information that is necessary to interpret observations of these gases. This will help us to assess where, when, and how compounds found in the coma, such as  $O_2$  [13], formed — on the surface of cometary nucleus, on dust grains in the protosolar nebula, or elsewhere?

In order to be able to assess what processes are active on the surface we need to know the fluxes of energetic neutrals and ions onto it. This will enable modelling of the effect of sputtering on the surface, and it is also needed to infer surface composition from observations of sputtered or otherwise released or created material. Measuring the flux of electrons to and from the surface will enable us to determine the surface charge, and this quantity also affects dust levitation through charging.

## **5.3 Dust-plasma interactions**

Dust in the coma interacts with the plasma charging the dust grains either positively or negatively. Dust motion in the coma is affected by both dust grain and plasma properties, and dust grains may constitute a distributed source of gas emissions in the coma as was seen at comet 67P for the halogens [27]. While we know what forces can act on a dust grain, and the basic processes for charging of the grains are known, the behaviour is expected to be very different for different grain sizes and different plasma parameters. Therefore, we still need to ask a basic question.

### ⇒ **What is the role of charged dust in the coma?**

How is the dust distributed in space around a comet? The spatial distribution is affected by the electric fields, and if the dust content is sufficiently high, charged dust will have a significant effect on the electric field.

What are the size and charge distributions? As charging of grains can lead to fragmentation, the space and charge distributions provide information about the grains themselves.

How does the presence of dust affect the sources of neutral gas and plasma in the coma? If the dust density is high, outgassing from the grains may be a significant source of neutral gas. In that case, the motion of dust grains under the influence of electromagnetic forces may have an appreciable effect on neutral gas observations.

How do plasma waves interact with the dust? Observations of dust waves in the plasma can provide an indirect means of assessing the dust content in the coma.

Observations of nano-dust may be performed indirectly via electron, ion, and wave measurements; large grains may be observed optically; and intermediate grain sizes require dedicated dust detectors. Since spacecraft more often than not are charged to

a potential different from the ambient plasma, charged dust grains must overcome the potential barrier to reach the spacecraft and be detected. When the relative speed between the spacecraft and the comet is low, as in the Rosetta case, this represents a challenge in measuring the low energy dust, and it may require development of new experimental techniques. Possible directions for the development to take include putting a dust detector on a long boom on a spinning spacecraft, thereby increasing the detector to dust relative speed, or controlling the potential of the dust detector to enable the charged dust to reach it. The ability to correct for spacecraft potential fluctuations is valuable not only in dust detection, but also for accurate measurements of low energy electrons and ions.

## 6 Possible missions

In order to answer the science questions presented in Section 5, two aspects of space missions are particularly important: **conducting multi-point measurements** and **orbiting a comet for an extended period of time**. This is necessary to obtain the 3D structure, differentiate temporal and spatial variability, and simultaneously assess the variation in different plasma regions. Ideally, a mission should be able to do all of that to achieve the highest science return. We propose three different mission profiles that, at least partially, address the science questions. As can be seen from Table 1, only mission profile A is able to answer all science questions, whereas B and C focus on specific subsets.

**Table 1** Main science questions (see Section 5) and mission profiles (see Section 6) suggested to solve them

Science Question	Mission profile
How asymmetric are large-scale structures at comets?	A, B <sup>a</sup>
Which boundaries exist at a comet during its journey through the Solar System?	A, B
What are the processes behind the diamagnetic cavity formation? Is it different for 67P and 1P?	A, B <sup>b</sup> , C
What is the cause of tail disconnection events and tail rays?	A
What is the role of collisions in the densest part of the coma?	A, B, C
How do electric fields contribute to energy, momentum, and mass transfer in the plasma?	A
What is the role of the electrons as magnetic field carriers in a plasma where the ions are not magnetised?	A, C
How do waves and wave–particle interactions affect the cometary plasma?	A
How do the plasma and the nucleus interact?	A, B
What is the role of charged dust in the coma?	A, B

<sup>a</sup>Spacecraft I has to provide radial coverage

<sup>b</sup>Spacecraft I and II need to be in the boundary region at the same time

## 6.1 Mission profile A: multi-spacecraft mission

This mission follows a comet in the same way Rosetta did: it will rendezvous with a comet well before it reaches perihelion, and accompany it for as long as possible. The new concept compared to Rosetta is that it is optimized for plasma measurements and consists of several identical spacecraft and a mother spacecraft. This ensures that simultaneous, inter-comparable measurements at multiple points can be performed.

Although the number of spacecraft is theoretically unlimited, we suggest to have at least four in total, which enables us to use methods that have been tried and tested using missions such as Cluster, Themis, and MMS. For example, the curlometer technique can give 3D measurements of the current in the region between the spacecraft, a measurement that is important for almost all the science questions.

The trajectory at a comet is easily adjustable, as the gravitational field of the nucleus is very small and thus the flying configuration of the spacecraft can be changed regularly. This means that it can be switched from a tetrahedron (for the curlometer technique to determine 3D currents) to a pearls-on-a-string formation with large cometocentric distance variations, which is advantageous for measuring the oscillations along a boundary.

To answer the science questions, the following quantities need to be measured:

- 3D magnetic field
- 3D electric field
- plasma density, temperature, and heat flux
- ion velocity distribution function with mass resolution (at least protons/water/carbondioxide)
- ENAs
- electron velocity distribution function
- neutral gas density and major constituents
- dust flux
- visible light and UV images of nucleus and coma

Thus, the proposed instrument suite would include a scalar and vector magnetometer and an electric field instrument to measure the fields. An ion mass/energy spectrometer with an ENA detector and an electron energy spectrometer should then provide detailed moments of the particle distribution functions. To support the plasma measurements and in particular the monitoring of the interactions between the ionised and the neutral phases that form a cometary coma, a neutral gas pressure gauge, a visible light camera, and a UV camera should also be included. To support the monitoring of the interactions between the ionised and the dust phases, a nanodust detector should be included. All instruments have heritage from missions such as Rosetta, Venus Express, Mars Express, Cluster, Cassini, BepiColombo, and JUICE. However, new development is necessary to achieve the accuracies needed in some cases. For example, to assess the role of dust, the difference in ion and electron density must be determined even at low spacecraft speeds.

For calibration purposes and to cover the entire sky with the field of view, the spacecraft should be spinning. To enable measurements of the low energy ions, the spacecraft potential should be kept as close to zero as possible. This is challenging in

a plasma that is warm and dense, as is the case at a comet, therefore some further technological development in active spacecraft potential control is required. To optimise science return only the mother spacecraft could carry the remote observing instruments and high gain antenna, which means it should be three-axis stabilised. The spinning spacecraft would transmit their collected data to the three-axis stabilised one, which would handle communications with Earth. The radio-links between the spacecraft could also be used to measure the total electron content along a line between two spacecraft. Four spacecraft can be manoeuvred so that these lines of sight intersect, allowing tomographic analysis of the electron density.

## 6.2 Mission profile B: sub-spacecrafts within a cometary mission

For this mission profile we assume that a mission to explore a cometary nucleus is planned in the near future. We propose one or multiple sub-spacecraft (spacecraft II) to accompany a Rosetta type comet mission (orbiter, spacecraft I). Spacecraft I should provide communication with Earth as well as the main propulsion system for the cruise phase. One of the sub-spacecraft could be provided by an international partner as was done, for example, for Bepi-Colombo.

To enable multi-point measurements the orbiter should also be equipped with a suite of plasma instruments similar to that on Rosetta, i.e. a magnetometer, a Langmuir probe, and electron and ion sensors.

We propose one or multiple sub-spacecraft, dedicated to investigations of the plasma. This has the advantage that this spacecraft can also go to large cometocentric distances without impacting the main spacecraft's science goals. The instrument suite should be similar to that proposed in mission profile A. It is also assumed that spacecraft I is equipped with a neutral gas monitor and an imager for its main science goals. The assumption is that this spacecraft is as close as possible to the nucleus to enable detailed investigations of the surface.

## 6.3 Mission profile C: artificial comet

To investigate the fundamental properties of plasma physics, space could be used as a convenient, accessible, clean physics laboratory. For instance, the impact of heavy ions on a plasma flow can be directly investigated, in a controlled way, by creating an artificial comet near Earth. This has the advantage of high telemetry rates and low propulsion requirements. The spacecraft should be equipped with similar instruments as mission profile A with the addition of an assembly to deploy canisters of heavy atoms/molecules. The canisters are then exploded and the ionisation and subsequent incorporation of the heavy ions into the solar wind could be studied in more detail. In order to obtain multi-point measurements the release should be coordinated with other Earth-orbiting satellites so that these also pass through the cloud. There are currently several plasma-instrument carrying missions available, e. g. Cluster, THEMIS, and MMS. The event could also be observed remotely with either ground- or space-based telescopes.

Such an experiment would be very similar to the AMPTE mission, with the added advantage of existing infrastructure in the near-Earth solar wind and much improved

instruments on the main spacecraft. There is also a possibility of observing the artificial comet with telescopes from Earth with involvement of the amateur astronomy community. The choice of gas should also be adjusted to better reflect the ionisation rate at real comets, because Barium (used by AMPTE) has an ionisation frequency that is three orders of magnitude larger than that of water.

#### 6.4 Additional measurements

To support the three mission profiles other measurements will be beneficial. For example, laboratory measurements of charge exchange rates or collision rates are still needed to provide the input parameters for detailed models of the plasma. Energy-dependent collisional cross sections for low energy particles are of particular interest. Also, experiments on ice sublimating in a vacuum will aid the understanding of the development of dust grains containing a combination of ice and refractory materials.

Ground-based remote observations of plasma tails are needed to provide large scale context for the in-situ measurements. For ideal coverage the amateur astronomy community should be included. New telescopes, both on Earth and in space, will increase the detection rate for comets and provide an even larger catalogue of mission targets.

Simulations – multi-fluid MHD, hybrid, or fully kinetic on large scales – are needed to provide the necessary context to interpret the in situ observations.

### 7 Conclusions

Table 1 summarises the main science questions outlined in this White Paper. The investigation of the cometary plasma environment will not only provide new insights on the interaction of comets with the solar wind but can also be a useful vehicle to study the impact of small scale plasma processes on large scale structures. Of the three mission profiles shown here, the multi-point rendezvous mission (A) is needed to answer many of the questions that still remain. An addendum to this white paper discussing the relevance of the cometary plasma environment to other plasma environments may be found in Appendix A.

Especially after the unprecedented and unequalled success of the European missions to comets, Giotto and Rosetta, as well as the upcoming Comet Interceptor, we urge ESA to keep up their predominance in this sector of space research and include a cometary plasma mission in the Voyage 2050 program.

### Appendix A: Addendum

In the light of the White Papers that were submitted to ESA's Voyage 2050 call, and the presentations and discussions at the workshop held in October 2019 in Madrid, we, as authors of the White Paper on Cometary Plasma Science, would like to add a few points to our discourse. In the White Paper we argue that comets provide a laboratory for studies of the role of small scale plasma processes in large scale systems,

which is of general interest in physics and has implications for a wide range of situations in the Universe. We would like to highlight that the topic of the White Paper is strongly linked to a number of other Voyage 2050 submissions. Therefore, the lead author is a co-signatory of the joint statement “The Plasma Universe: A Coherent Science Theme for Voyage 2050”, by [147]. There are some additional aspects not stressed in the Cometary Plasma Science White Paper, where cometary plasma physics can have a major impact on Astronomy and Astrophysics.

An important topic in exoplanet research today is habitability, and the presence of an appropriate planetary atmosphere plays a key role for conditions for life since it is critical for a favourable climate and for maintaining liquid water on the surface. For life to evolve on a planet it is necessary that it remains habitable, and keeps a stable atmosphere, over long periods of time. From research on our own Solar System we know that interactions between the solar wind and the planetary environments have crucial impacts on atmospheric escape by which a planet’s atmosphere is gradually eroded [7, 17, 134]. The characteristics of plasma boundaries (e.g. ionopause, magnetopause, and bow shock) strongly affect the interaction of the planetary environment with the stellar wind [158]. Important escape processes, like sputtering and ion pickup that together dominate the escape from Venus, are highly dependent on the position of these boundaries [66]. Comets hold the key to the understanding of boundary formation on a fundamental level, and they also enable us to explore parameter regimes that are unavailable at planets in our Solar System by going through a wide range of parameters on their journey through the Solar System [65, 138]. Both these aspects can be used to make extrapolations to situations at planets orbiting other stars.

Considering the evolution of a planet (in our own Solar System or elsewhere) and its ability to hold on to its water, it is of particular interest to study the interaction of stellar winds with water-rich exospheres. Comets provide exactly that kind of environment, where water is the dominating particle species in the coma most of the time (see for example [74] for a Rosetta observation). As outlined in the White Paper, there is an intricate combination of collisional and non-collisional interaction processes in the regions where the solar wind passes through the water-dominated atmosphere.

We would also like to stress that to answer the outstanding questions in comet plasma physics requires simultaneous measurements by several spacecraft that accompany a comet for an extended period of time. It is a general problem in experimental space physics that one cannot distinguish between spatial and temporal effects from single-point observations. So far, all in-situ observations ever made at comets have been performed at one single point in space. The Comet Interceptor mission, which is now under development by ESA with a subspacespacecraft provided by JAXA, will be pioneering in that it is the first mission to provide multi-point measurements at a comet. However, as a Fast-class mission with a small budget, it is also limited, and it cannot replace a multi-point comet companion mission. This is due in part to its extremely sparse plasma instrumentation, not all subspacespacecraft carry a full set of plasma instruments, and in part to the mission being a fast flyby, which cannot provide more than a snapshot of the comet plasma in one single spacecraft formation and for one single heliocentric distance and outgassing rate. The mission concepts we outline in the White Paper will therefore constitute a major advance in plasma science, and thus impact the understanding of a wide range of plasma physical contexts in space and astrophysics.

**Acknowledgements** C. G. is supported by an ESA Research Fellowship. H. G. acknowledges support by the Swedish National Space Agency grant 108/18. B. S.-C. acknowledges support through UK-STFC grant ST/S000429/1. French co-authors acknowledge the support of CNES for the Rosetta and Comet Interceptor missions. I. M. acknowledges support through grants of Research Council of Norway (262941 and 275503).

## References

1. Alfvén, H.: On the origin of the solar system. Oxford University Press, Oxford (1954)
2. Alfvén, H.: On the theory of comet tails. *Tellus* **9** (1957)
3. Alho, M., Simon Wedlund, C., Nilsson, H., Kallio, E., Jarvinen, R., Pulkkinen, T.: Hybrid modelling of cometary plasma environments. II. Remote sensing of a cometary bow shock. *A&A* **1**. <https://doi.org/10.1093/mnras/stx868> (2019)
4. André, M., Odelstad, E., Graham, D.B., Eriksson, A.I., Karlsson, T., Stenberg Wieser, G., Vigren, E., Norgren, C., Johansson, F.L., Henri, P., Rubin, M., Richter, I.: Lower hybrid waves at comet 67P/Churyumov-Gerasimenko. *Mon. Not. Royal Astron. Soc.* **469**, S29–S38 (2017). <https://doi.org/10.1093/mnras/stx868>
5. Auster, H.U., Apathy, I., Berghofer, G., Fornacon, K.H., Remizov, A., Carr, C., Güttler, C., Haerendel, G., Heinisch, P., Hercik, D., Hilchenbach, M., Kühr, E., Magnes, W., Motschmann, U., Richter, I., Russell, C.T., Przyklenk, A., Schwingenschuh, K., Sierks, H., Glassmeier, K.H.: The nonmagnetic nucleus of comet 67P/Churyumov-Gerasimenko. *Science* **349**(1), 015102 (2015). <https://doi.org/10.1093/mnras/stx868>
6. Bale, S.D., Balikhin, M.A., Horbury, T.S., Krasnoselskikh, V.V., Kucharek, H., Möbius, E., Walker, S.N., Balogh, A., Burgess, D., Lembège, B., Lucek, E.A., Scholer, M., Schwartz, S.J., Thomsen, M.F.: Quasi-perpendicular shock structure and processes. *Space Sci. Rev.* **118**(1), 161–203 (2005). <https://doi.org/10.1093/mnras/stx868>
7. Barabash, S., Fedorov, A., Sauvaud, J.J., Lundin, R., Russell, C.T., Futaana, Y., Zhang, T.L., Andersson, H., Brinkfeldt, K., Grigoriev, A., Holmström, M., Yamauchi, M., Asamura, K., Baumjohann, W., Lammer, H., Coates, A.J., Kataria, D.O., Linder, D.R., Curtis, C.C., Hsieh, K.C., Sandel, B.R., Grande, M., Gunell, H., Koskinen, H.E.J., Kallio, E., Riihelä, P., Sälens, T., Schmidt, W., Kozyra, J., Krupp, N., Fränz, M., Woch, J., Luhmann, J., McKenna-Lawlor, S., Mazelle, C., Thocaven, J.J., Orsini, S., Cerulli-Irelli, R., Mura, M., Milillo, M., Maggi, M., Roelof, E., Brandt, P., Szego, K., Winningham, J.D., Frahm, R.A., Scherrer, J., Sharber, J.R., Wurz, P., Bochsler, P.: The loss of ions from Venus through the plasma wake. *Nature* **450**(7170), 650–653 (2007). <https://doi.org/10.1038/nature06434>
8. Barkan, A., Merlino, R.L., D’Angelo, N.: Laboratory observation of the dust-acoustic wave mode. *Phys. Plasmas* **2**, 3563–3565 (1995). <https://doi.org/10.1093/mnras/stx868>
9. Behar, E., Nilsson, H., Alho, M., Goetz, C., Tsurutani, B.: The birth and growth of a solar wind cavity around a comet - Rosetta observations. *MNRAS* **469**, S396–S403 (2017). <https://doi.org/10.1093/mnras/stx868>
10. Beth, A., Galand, M.: Effects of the convective field on weakly outgassing comets. *Mon. Not. Royal Astron. Soc.* **469**, S824–S841 (2018). <https://doi.org/10.1093/mnras/stx868>
11. Beth, A., Altwegg, K., Balsiger, H., Berthelier, J.-J., Calmonte, U., Combi, M.R., De Keyser, J., Dhoooge, F., Fiethe, B., Fuselier, S.A., Galand, M., Gasc, S., Gombosi, T.I., Hansen, K.C., Hässig, M., Heritier, K.L., Kopp, E., Le Roy, L., Mandt, K.E., Peroy, S., Rubin, M., Sémon, T., Tzou, C.-Y., Vigren, E.: First in situ detection of the cometary ammonium ion  $\text{NH}_4^+$  (protonated ammonia  $\text{NH}_3$ ) in the coma of 67P/C-G near perihelion. *Mon. Not. Royal Astron. Soc.* **462**(Suppl.1), S562–S572 (2016)
12. Beth, A., Galand, M., Heritier, K.: Comparative study of photo-produced ionosphere in the close environment of comets. *A&A* in press. <https://doi.org/10.1051/0004-6361/201833517> (2018)
13. Bieler, A., Altwegg, K., Balsiger, H., Bar-Nun, A., Berthelier, J.J., Bochsler, P., Briois, C., Calmonte, U., Combi, M., De Keyser, J., van Dishoeck, E.F., Fiethe, B., Fuselier, S.A., Gasc, S., Gombosi, T.I., Hansen, K.C., Hässig, M., Jäckel, A., Kopp, E., Korth, A., Le Roy, L., Mall, U., Maggiolo, R., Marty, B., Mousis, O., Owen, T., Rème, H., Rubin, M., Sémon, T., Tzou, C.Y., Waite, J.H., Walsh, C.,



- Wurz, P.: Abundant molecular oxygen in the coma of comet 67p/churyumov-Gerasimenko. *Nature* **526**, 678–681 (2015). <https://doi.org/10.1093/mnras/stx868>
14. Biermann, L.: Kometenschweife und solare Korpuskularstrahlung. *Zeitschrift für Astrophysik* **29**, 274 (1951)
  15. Biermann, L., Brosowski, B., Schmidt, H.U.: The interactions of the solar wind with a comet. *Sol. Phys.* **1**, 254–284 (1967). <https://doi.org/10.1093/mnras/stx868>
  16. Boice, D.C., Goldstein, R., Schulz, R.: A cometary perspective of Enceladus. In: Fernández, J.A., Lazzaro, D., Prialnik, D. (eds.) *IAU Symposium*, vol. 263, pp. 151–156 (2010). <https://doi.org/10.1093/mnras/stx868>
  17. Brain, D.A., Bagenal, F., Ma, Y.J., Nilsson, H., Stenberg Wieser, G.: Atmospheric escape from unmagnetized bodies. *J. Geophys. Res. (Planets)* **121**(12), 2364–2385 (2016). <https://doi.org/10.1093/mnras/stx868>
  18. Breuillard, H., Henri, P., Bucciantini, L., Volwerk, M., Karlsson, T., Eriksson, A., Johansson, F., Odelstad, E., Richter, I., Goetz, C., Vallières, X., Hajra, R.: The properties of the singing comet waves in the 67P/Churyumov–Gerasimenko plasma environment as observed by the Rosetta mission. *A&A*. <https://doi.org/10.1051/0004-6361/201834876> (2019)
  19. Broiles, T.W., Burch, J.L., Chae, K., Clark, G., Cravens, T.E., Eriksson, A., Fuselier, S.A., Frahm, R.A., Gasc, S., Goldstein, R., Henri, P., Koenders, C., Livadiotis, G., Mandt, K.E., Mokashi, P., Nemeth, Z., Odelstad, E., Rubin, M., Samara, M.: Statistical analysis of suprathermal electron drivers at 67P/Churyumov- Gerasimenko. *MNRAS* **462**, S312–S322 (2016). <https://doi.org/10.1093/mnras/stx868>
  20. Burch, J.L., Gombosi, T.I., Clark, G., Mokashi, P., Goldstein, R.: Observation of charged nanograins at comet 67p/churyumov-Gerasimenko. *Geophys. Res. Lett.* **42**(16), 6575–6581 (2015). <https://doi.org/10.1093/mnras/stx868>
  21. Coates, A.J.: Heavy ion effects on cometary shocks. *Adv. Space Res.* **15**(8-9), 403–413 (1995). <https://doi.org/10.1093/mnras/stx868>
  22. Coates, A.J., Jones, G.H.: Plasma environment of Jupiter family comets. *Planet. Space Sci.* **57**, 1175–1191 (2009). <https://doi.org/10.1093/mnras/stx868>
  23. Cravens, T.E.: The physics of the cometary contact surface. In: Battrick, B., Rolfe, E.J., Reinhard, R. (eds.) *ESLAB Symposium on the Exploration of Halley's Comet*, vol. 250, p. 241 (1986)
  24. Cravens, T.E.: Theory and observations of cometary ionospheres. *Adv. Space Res.* **7**, 147–158 (1987). <https://doi.org/10.1093/mnras/stx868>
  25. Cravens, T.E.: Galactic cosmic rays and cell-hit frequencies outside the magnetosphere. *Adv. Space Res.* **9**(10), 293–298 (1989). <https://doi.org/10.1093/mnras/stx868>
  26. Cravens, T.E.: Comet Hyakutake x-ray source: Charge transfer of solar wind heavy ions. *Geophys. Res. Lett.* **24**, 105–108 (1997). <https://doi.org/10.1093/mnras/stx868>
  27. De Keyser, J., Dhooghe, F., Altwegg, K., Balsiger, H., Berthelier, J.J., Briois, C., Calmonte, U., Cessateur, G., Combi, M.R., Equeter, E., Fiethe, B., Fuselier, S., Gasc, S., Gibbons, A., Gombosi, T., Gunell, H., Hässig, M., Le Roy, L., Maggiolo, R., Mall, U., Marty, B., Neefs, E., Rème, H., Rubin, M., Sémon, T., Tzou, C.Y., Wurz, P.: Evidence for distributed gas sources of hydrogen halides in the coma of comet 67p/churyumov-Gerasimenko. *Mon. Not. Royal Astron. Soc.* **469**, S695–S711 (2017). <https://doi.org/10.1093/mnras/stx868>
  28. Deca, J., Divin, A., Henri, P., Eriksson, A., Markidis, S., Olshevsky, V., Horányi, M.: Electron and ion dynamics of the solar wind interaction with a weakly outgassing comet. *Phys. Rev. Lett.* **118**, 205101 (2017). <https://doi.org/10.1093/mnras/stx868>
  29. Deca, J., Henri, P., Divin, A., Eriksson, A., Galand, M., Beth, A., Ostaszewski, K., Horányi, M.: Building a weakly outgassing comet from a generalized ohm's law. *Phys. Rev. Lett.* **123**(5), 055101 (2019). <https://doi.org/10.1093/mnras/stx868>
  30. Delva, M., Bertucci, C., Volwerk, M., Lundin, R., Mazelle, C., Romanelli, N.: Upstream proton cyclotron waves at venus near solar maximum. *JGeophysRes (Space Physics)* **120**(1), 344–354 (2015). <https://doi.org/10.1093/mnras/stx868>
  31. Dennerl, K.: Charge transfer reactions. *Space Sci Rev* **157**, 57–91 (2010). <https://doi.org/10.1093/mnras/stx868>
  32. Dhooghe, F., De Keyser, J., Altwegg, K., Briois, C., Balsiger, H., Berthelier, J.J., Calmonte, U., Cessateur, G., Combi, M.R., Equeter, E., Fiethe, B., Fray, N., Fuselier, S., Gasc, S., Gibbons, A., Gombosi, T., Gunell, H., Hässig, M., Hilchenbach, M., Le Roy, L., Maggiolo, R., Mall, U., Marty, B., Neefs, E., Rème, H., Rubin, M., Sémon, T., Tzou, C.Y., Wurz, P.: Halogens as tracers of protosolar

- nebula material in comet 67P/Churyumov-Gerasimenko. *Mon. Not. Royal Astron. Soc.* **472**, 1336–1345 (2017). <https://doi.org/10.1093/mnras/stx868>
33. Eastwood, J.P., Lucek, E.A., Mazelle, C., Meziane, K., Narita, Y., Pickett, J., Treumann, R.A.: The foreshock. *Space Sci. Rev.* **118**(1), 41–94 (2005). <https://doi.org/10.1093/mnras/stx868>
  34. Edberg, N.J.T., Eriksson, A.I., Odelstad, E., Henri, P., Lebreton, J.P., Gasc, S., Rubin, M., André, M., Gill, R., Johansson, E.P.G., Johansson, F., Vigren, E., Wahlund, J.E., Carr, C.M., Cupido, E., Glassmeier, K.H., Goldstein, R., Koenders, C., Mandt, K., Nemeth, Z., Nilsson, H., Richter, I., Wieser, G.S., Szego, K., Volwerk, M.: Spatial distribution of low-energy plasma around comet 67P/CG from Rosetta measurements. *Geophys. Res. Lett.* **42**, 4263–4269 (2015). <https://doi.org/10.1002/2015GL064233>, arXiv:1608.06745
  35. Edberg, N.J.T., Alho, M., André, M., Andrews, D.J., Behar, E., Burch, J.L., Carr, C.M., Cupido, E., Engelhardt, I.A.D., Eriksson, A.I., Glassmeier, K.H., Goetz, C., Goldstein, R., Henri, P., Johansson, F.L., Koenders, C., Mandt, K., Möstl, C., Nilsson, H., Odelstad, E., Richter, I., Simon Wedlund, C., Stenberg Wieser, G., Szego, K., Vigren, E., Volwerk, M.: CME Impact on comet 67P/Churyumov-Gerasimenko. *MNRAS* **462**, S45–S56 (2016). <https://doi.org/10.1093/mnras/stx868>
  36. Ekenbäck, A., Holmström, M., Barabash, S., Gunell, H.: Energetic neutral atom imaging of comets. *GeophysResLett* **35**, L05103 (2008). <https://doi.org/10.1093/mnras/stx868>
  37. Engelhardt, I., Wahlund, J.E., Andrews, D., Eriksson, A., Ye, S., Kurth, W., Gurnett, D., Morooka, M., Farrell, W., Dougherty, M.: Plasma regions, charged dust and field-aligned currents near Enceladus. *Planet. Space Sci.* **117**, 453–469 (2015). <https://doi.org/10.1093/mnras/stx868>
  38. Engelhardt, I.A.D., Eriksson, A.I., Vigren, E., Vallières, X., Rubin, M., Gilet, N., Henri, P.: Cold electrons at comet 67P/Churyumov-Gerasimenko. *A&A* **616**, A51 (2018). <https://doi.org/10.1093/mnras/stx868>
  39. Eriksson, A.I., Engelhardt, I.A.D., André, M., Boström, R., Edberg, N.J.T., Johansson, F.L., Odelstad, E., Vigren, E., Wahlund, J.E., Henri, P., Lebreton, J.P., Miloch, W.J., Paulsson, J.J.P., Simon Wedlund, C., Yang, L., Karlsson, T., Jarvinen, R., Broiles, T., Mandt, K., Carr, C.M., Galand, M., Nilsson, H., Norberg, C.: Cold and warm electrons at comet 67P/Churyumov-Gerasimenko. *A&A* **605**, A15 (2017). <https://doi.org/10.1093/mnras/stx868>
  40. Ershkovich, A.I., Flammer, K.R.: Nonlinear stability of the dayside cometary ionopause. *Astrophys J* **328**, 967–973 (1988). <https://doi.org/10.1093/mnras/stx868>
  41. Ershkovich, A.I., Mendis, D.A.: Effects of the interaction between plasma and neutrals on the stability of the cometary ionopause. *Astrophys J* **302**, 849–852 (1986). <https://doi.org/10.1093/mnras/stx868>
  42. Fulle, M., Marzari, F., Corte, V.D., Fornasier, S., Sierks, H., Rotundi, A., Barbieri, C., Lamy, P.L., Rodrigo, R., Koschny, D., Rickman, H., Keller, H.U., López-Moreno, J.J., Accolla, M., Agarwal, J., A'Hearn, M.F., Altobelli, N., Barucci, M.A., Bertaux, J.L., Bertini, I., Bodewits, D., Bussolletti, E., Colangeli, L., Cosi, M., Cremonese, G., Crifo, J.F., Deppo, V.D., Davidsson, B., Debei, S., Cecco, M.D., Esposito, F., Ferrari, M., Giovane, F., Gustafson, B., Green, S.F., Groussin, O., Grün, E., Gutierrez, P., Güttler, C., Herranz, M.L., Hviid, S.F., Ip, W., Ivanovski, S.L., Jerónimo, J.M., Jorda, L., Knollenberg, J., Kramm, R., Kührt, E., Küppers, M., Lara, L., Lazzarin, M., Leese, M.R., López-Jiménez, A.C., Lucarelli, F., Epifani, E.M., McDonnell, J.A.M., Mennella, V., Molina, A., Morales, R., Moreno, F., Mottola, S., Naletto, G., Ockay, N., Ortiz, J.L., Palomba, E., Palumbo, P., Perrin, J.M., Rietmeijer, F.J.M., Rodríguez, J., Sordini, R., Thomas, N., Tubiana, C., Vincent, J.B., Weissman, P., Wenzel, K.P., Zakharov, V., Zarnecki, J.C.: Evolution of the dust size distribution of comet 67p/churyumov-gerasimenko from 2.2 au to perihelion. *Astrophys. J.* **821**(1), 19 (2016). <https://doi.org/10.1093/mnras/stx868>
  43. Fuselier, S.A., Funsten, H.O., Heitzler, D., Janzen, P., Kucharek, H., McComas, D.J., Möbius, E., Moore, T.E., Petrinec, S.M., Reisenfeld, D.B., Schwadron, N.A., Trattner, K.J., Wurz, P.: Energetic neutral atoms from the Earth's subsolar magnetopause. *Geophys. Res. Lett.* **37**, L13101 (2010). <https://doi.org/10.1029/2010GL044140>
  44. Fuselier, S.A., Altwegg, K., Balsiger, H., Berthelier, J.J., Bieler, A., Briois, C., Broiles, T.W., Burch, J.L., Calmonte, U., Cessateur, G., Combi, M., De Keyser, J., Fiethe, B., Galand, M., Gasc, S., Gombosi, T.I., Gunell, H., Hansen, K.C., Hässig, M., Jäckel, A., Korth, A., Le Roy, L., Mall, U., Mandt, K.E., Petrinec, S.M., Raghuram, S., Rème, H., Rinaldi, M., Rubin, M., Sémon, T., Trattner, K.J., Tzou, C.Y., Vigren, E., Waite, J.H., Wurz, P.: ROSINA/DFMS And IES observations of 67P: Ion-neutral chemistry in the coma of a weakly outgassing comet. *Astron. Astrophys.* **583**, A2 (2015). <https://doi.org/10.1093/mnras/stx868>

45. Fuselier, S.A., Altwegg, K., Balsiger, H., Berthelier, J.J., Beth, A., Bieler, A., Briois, C., Broiles, T.W., Burch, J.L., Calmonte, U., Cessateur, G., Combi, M., De Keyser, J., Fiethe, B., Galand, M., Gasc, S., Gombosi, T.I., Gunell, H., Hansen, K.C., Hässig, M., Heritier, K.L., Korth, A., Le Roy, L., Luspai-Kuti, A., Mall, U., Mandt, K.E., Petrinec, S.M., Rème, H., Rinaldi, M., Rubin, M., Sémon, T., Trattner, K.J., Tzou, C.Y., Vigren, E., Waite, J.H., Wurz, P.: Ion chemistry in the coma of comet 67P near perihelion. *Mon. Not. Royal Astron. Soc.* **462**, S67–S77 (2016). <https://doi.org/10.1093/mnras/stx868>
46. Futaana, Y., Barabash, S., Grigoriev, A., Holmström, M., Kallio, E., Brandt, P.C., Gunell, H., Brinkfeldt, K., Lundin, R., Andersson, H., Yamauchi, M., McKenna-Lawler, S., Winningham, J.D., Frahm, R.A., Sharber, J.R., Scherrer, J., Coates, A.J., Linder, D.R., Kataria, D.O., Säles, T., Riihela, P., Schmidt, W., Koskinen, H., Kozyra, J., Luhmann, J., Roelof, E., Williams, D., Livi, S., Curtis, C.C., Hsieh, K., Sandel, B.R., Grande, M., Carter, M., Sauvaud, J.A., Fedorov, A., Thocaven, J.J., Orsini, S., Cerulli-Irelli, R., Maggi, M., Wurz, P., Bochsler, P., Krupp, N., Woch, J., Fränz, M., Asamura, K., Dierker, C.: First ENA observations at Mars: Subsolar ENA jet. *Icarus* **182**, 413–423 (2006a). <https://doi.org/10.1093/mnras/stx868>
47. Futaana, Y., Barabash, S., Grigoriev, A., Winningham, D., Frahm, R., Yamauchi, M., Lundin, R.: Global response of Martian plasma environment to an interplanetary structure: From ena and plasma observations at Mars. *Space Sci. Rev.* **126**(1–4), 315–332 (2006b). <https://doi.org/10.1093/mnras/stx868>
48. Galand, M., Héritier, K.L., Odelstad, E., Henri, P., Broiles, T.W., Allen, A.J., Altwegg, K., Beth, A., Burch, J.L., Carr, C.M., Cupido, E., Eriksson, A.I., Glassmeier, K.H., Johansson, F.L., Lebreton, J.P., Mandt, K.E., Nilsson, H., Richter, I., Rubin, M., Sagnières, L.B.M., Schwartz, S.J., Sémon, T., Tzou, C.Y., Vallières, X., Vigren, E., Wurz, P.: Ionospheric plasma of comet 67P probed by Rosetta at 3 au from the Sun. *MNRAS* **462**, S331–S351 (2016). <https://doi.org/10.1093/mnras/stx868>
49. Galeev, A.A., Cravens, T.E., Gombosi, T.I.: Solar wind stagnation near comets. *ApJ* **289**, 807–819 (1985). <https://doi.org/10.1093/mnras/stx868>
50. Galeev, A.A., Gringauz, K.I., Klimov, S.I., Remizov, A.P., Sagdeev, R.Z., Savin, S.P., Sokolov, A.Y., Verigin, M.I., Szegő, K., Tátrallyay, M.: Physical processes in the vicinity of the cometopause interpreted on the basis of plasma, magnetic field, and plasma wave data measured on board the vega 2 spacecraft. *J. Geophys. Res.* **93**(A7), 7527–7531 (1988). <https://doi.org/10.1029/JA093iA07p07527>
51. Gan, L., Cravens, T.E.: Electron energetics in the inner coma of Comet Halley. *J. Geophys. Res.* **95**, 6285–6303 (1990). <https://doi.org/10.1093/mnras/stx868>
52. Gilet, N., Henri, P., Wattieaux, G., Cilibrasi, M., Béghin, C.: Electrostatic potential radiated by a pulsating charge in a Two-Electron temperature plasma. *Radio Sci.* **52**, 1432–1448 (2017). <https://doi.org/10.1093/mnras/stx868>
53. Glassmeier, K., Coates, A.J., Acuña, M.H., Goldstein, M.L., Johnstone, A.D., Neubauer, F.M., Rème, H.: Spectral characteristics of low-frequency plasma turbulence upstream of comet P/Halley. *J. Geophys. Res.* **94**, 37–48 (1989)
54. Glassmeier, K.H., Neubauer, F.M.: Low-frequency electromagnetic plasma waves at comet p/grigg-Skjellerup: Overview and spectral characteristics. *J. Geophys. Res.* **98**(A12), 20921–20936 (1993). <https://doi.org/10.1093/mnras/stx868>
55. Glassmeier, K.H., Motschmann, U., Mazelle, C., Neubauer, F.M., Sauer, K., Fuselier, S.A., Acuña, M.H.: Mirror modes and fast magnetoacoustic waves near the magnetic pileup boundary of comet P/Halley. *J. Geophys. Res.* **98**(A12), 20955–20964 (1993). <https://doi.org/10.1093/mnras/stx868>
56. Glassmeier, K.H., Boehnhardt, H., Koschny, D., Kührt, E., Richter, I.: The rosetta mission: Flying towards the origin of the solar system. *Space Sci. Rev.* **128**, 1–21 (2007). <https://doi.org/10.1093/mnras/stx868>
57. Gloeckler, G., Geiss, J., Schwadron, N.A., Fisk, L.A., Zurbuchen, T.H., Ipavich, F.M., von Steiger, R., Balsiger, H., Wilken, B.: Interception of comet Hyakutake's ion tail at a distance of 500 million kilometres. *Nature* **404**(6778), 576–578 (2000). <https://doi.org/10.1093/mnras/stx868>
58. Goetz, C., Koenders, C., Hansen, K.C., Burch, J., Carr, C., Eriksson, A., Frühauff, D., Güttler, C., Henri, P., Nilsson, H., Richter, I., Rubin, M., Sierks, H., Tsurutani, B., Volwerk, M., Glassmeier, K.H.: Structure and evolution of the diamagnetic cavity at comet 67P/Churyumov-Gerasimenko. *MNRAS* **462**, S459–S467 (2016a). <https://doi.org/10.1093/mnras/stx868>
59. Goetz, C., Koenders, C., Richter, I., Altwegg, K., Burch, J., Carr, C., Cupido, E., Eriksson, A., Güttler, C., Henri, P., Mokashi, P., Nemeth, Z., Nilsson, H., Rubin, M., Sierks, H., Tsurutani,

- B., Vallat, C., Volwerk, M., Glassmeier, K.H.: First detection of a diamagnetic cavity at comet 67P/Churyumov-Gerasimenko. *A&A* **588**, A24 (2016b). <https://doi.org/10.1093/mnras/stx868>
60. Goetz, C., Volwerk, M., Richter, I., Glassmeier, K.H.: Evolution of the magnetic field at comet 67P/Churyumov-Gerasimenko. *MNRAS* **469**, S268–S275 (2017). <https://doi.org/10.1093/mnras/stx868>
  61. Gombosi, T.I.: Charge exchange avalanche at the cometopause. *Geophys. Res. Lett.* **14**(11), 1174–1177 (1987). <https://doi.org/10.1093/mnras/stx868>
  62. Götz, C.: The plasma environment of comet 67P/Churyumov-Gerasimenko. PhD thesis, Technische Universität Braunschweig. <https://doi.org/10.1093/mnras/stx868> (2019)
  63. Gunell, H., Goetz, C., Eriksson, A., Nilsson, H., Simon Wedlund, C., Henri, P., Maggiolo, R., Hamrin, M., De Keyser, J., Rubin, M., Stenberg Wieser, G., Cessateur, G., Dhooghe, F., Gibbons, A.: Plasma waves confined to the diamagnetic cavity of comet 67P/Churyumov-Gerasimenko. *MNRAS* **469**, S84–S92 (2017a). <https://doi.org/10.1093/mnras/stx868>
  64. Gunell, H., Nilsson, H., Hamrin, M., Eriksson, A., Odelstad, E., Maggiolo, R., Henri, P., Vallières, X., Altwegg, K., Tzou, C.Y., Rubin, M., Glassmeier, K.H., Stenberg Wieser, G., Simon Wedlund, C., De Keyser, J., Dhooghe, F., Cessateur, G., Gibbons, A.: Ion acoustic waves at comet 67P/Churyumov-Gerasimenko – Observations and computations. *Astron. Astrophys.* **600**, A3 (2017b). <https://doi.org/10.1093/mnras/stx868>
  65. Gunell, H., Goetz, C., Simon Wedlund, C., Lindkvist, J., Hamrin, M., Nilsson, H., Llera, K., Eriksson, A., Holmström, M.: The infant bow shock: a new frontier at a weak activity comet. *A&A* **619**, L2 (2018a). <https://doi.org/10.1093/mnras/stx868>
  66. Gunell, H., Maggiolo, R., Nilsson, H., Stenberg, Wieser, G., Slapak, R., Lindkvist, J., Hamrin, M., De Keyser, J.: Why an intrinsic magnetic field does not protect a planet against atmospheric escape. *Astron. Astrophys.* **614**, L3 (2018b). <https://doi.org/10.1093/mnras/stx868>
  67. Gunell, H., Lindkvist, J., Goetz, C., Nilsson, H., Hamrin, M.: Polarisation of a small-scale cometary plasma environment: Particle-in-cell modelling of comet 67p/churyumov-Gerasimenko. *Astron. Astrophys.* **631**, A174 (2019). <https://doi.org/10.1093/mnras/stx868>
  68. Häberli, R.M., Gombosi, T.I., DeZeeuw, D.L., Combi, M.R., Powell, K.G.: Modeling of cometary x-rays caused by solar wind minor ions. *Science* **276**, 939–942 (1997). <https://doi.org/10.1093/mnras/stx868>
  69. Haerendel, G., Paschmann, G., Baumjohann, W., Carlson, C.W.: Dynamics of the AMPTE artificial comet. *Nature* **320**, 720–723 (1986). <https://doi.org/10.1093/mnras/stx868>
  70. Haider, S., Bhardwaj, A.: Radial distribution of production rates, loss rates and densities corresponding to ion masses ~40 amu in the inner coma of comet halley: Composition and chemistry. *Icarus* **177**(1), 196–216 (2005). <https://doi.org/10.1093/mnras/stx868>
  71. Hajra, R., Henri, P., Myllys, M., Héritier, K.L., Galand, M., Simon, Wedlund, C., Breuillard, H., Behar, E., Edberg, N.J.T., Goetz, C., Nilsson, H., Eriksson, A.I., Goldstein, R., Tsurutani, B.T., Moré, J., Vallières, X., Wattieaux, G.: Cometary plasma response to interplanetary corotating interaction regions during 2016 June–September: a quantitative study by the Rosetta Plasma Consortium. *MNRAS* **480**, 4544–4556 (2018). <https://doi.org/10.1093/mnras/stx868>
  72. Hall, B.E.S., Lester, M., Sánchez-Cano, B., Nichols, J.D., Andrews, D.J., Edberg, N.J.T., Opgenoorth, H.J., Fränz, M., Holmström, M., Ramstad, R., Witasse, O., Cartacci, M., Cicchetti, A., Noschese, R., Orosei, R.: Annual variations in the martian bow shock location as observed by the Mars Express mission. *JGeophysRes (Space Physics)* **121**(11). <https://doi.org/10.1093/mnras/stx868> (2016)
  73. Hansen, K.C., Altwegg, K., Berthelier, J.J., Bieler, A., Biver, N., Bockelée-Morvan, D., Calmonte, U., Capaccioni, F., Combi, M.R., De Keyser, J., Fiethe, B., Fougere, N., Fuselier, S.A., Gasc, S., Gombosi, T.I., Huang, Z., Le Roy, L., Lee, S., Nilsson, H., Rubin, M., Shou, Y., Snodgrass, C., Tensheev, V., Toth, G., Tzou, C.Y., Simon Wedlund, C., Team, Rosina.: Evolution of water production of 67P/Churyumov-Gerasimenko: An empirical model and a multi-instrument study. *MNRAS* **462**, S491–S506 (2016). <https://doi.org/10.1093/mnras/stx868>
  74. Hässig, M., Altwegg, K., Balsiger, H., Bar-Nun, A., Berthelier, J.J., Bieler, A., Bochsler, P., Briosis, C., Calmonte, U., Combi, M., De Keyser, J., Eberhardt, P., Fiethe, B., Fuselier, S.A., Galand, M., Gasc, S., Gombosi, T.I., Hansen, K.C., Jäckel, A., Keller, H.U., Kopp, E., Korth, A., Kühr, E., Le Roy, L., Mall, U., Marty, B., Mousis, O., Neefs, E., Owen, T., Rème, H., Rubin, M., Sémon, T., Tornow, C., Tzou, C.Y., Waite, J.H., Wurz, P.: Time variability and heterogeneity in the coma of 67P/Churyumov-Gerasimenko. *Science* **347**, aaa0276 (2015). <https://doi.org/10.1126/science.aaa0276>

75. Heinrich, J., Kim, S.H., Merlino, R.L.: Laboratory observations of self-excited dust acoustic shocks. *Phys. Rev. Lett.* **103**(11), 115002 (2009). <https://doi.org/10.1093/mnras/stx868>
76. Henri, P., Vallières, X., Hajra, R., Goetz, C., Richter, I., Glassmeier, K.H., Galand, M., Rubin, M., Eriksson, A.I., Nemeth, Z., Vigren, E., Beth, A., Burch, J.L., Carr, C., Nilsson, H., Tsurutani, B., Wattiaux, G.: Diamagnetic region(s): structure of the unmagnetized plasma around Comet 67p/CG. *MNRAS* **469**, S372–S379 (2017). <https://doi.org/10.1093/mnras/stx868>
77. Heritier, K.L., Altwegg, K., Balsiger, H., Berthelier, J.J., Beth, A., Bieler, A., Biver, N., Calmonte, U., Combi, M.R., De Keyser, J., Eriksson, A.I., Fiethe, B., Fougere, N., Fuselier, S.A., Galand, M., Gasc, S., Gombosi, T.I., Hansen, K.C., Hassig, M., Kopp, E., Odelstad, E., Rubin, M., Tzou, C.Y., Vigren, E., Vuitton, V.: Ion composition at comet 67P, near perihelion: Rosetta observations and model-based interpretation. *Mon. Notice R. Astron. Soc.* **469**(Suppl.2), S427–S442 (2017a). <https://doi.org/10.1093/mnras/stx868>
78. Heritier, K.L., Henri, P., Vallières, X., Galand, M., Odelstad, E., Eriksson, A.I., Johansson, F.L., Altwegg, K., Behar, E., Beth, A., Broiles, T.W., Burch, J.L., Carr, C.M., Cupido, E., Nilsson, H., Rubin, M., Vigren, E.: Vertical structure of the near-surface expanding ionosphere of comet 67P probed by Rosetta. *MNRAS* **469**, S118–S129 (2017b). <https://doi.org/10.1093/mnras/stx1459>
79. Heritier, K.L., Altwegg, K., Berthelier, J.J., Beth, A., Carr, C.M., D Keyser, J., Eriksson, A.I., Fuselier, S.A., Galand, M., Gombosi, T.I., Henri, P., Johansson, F.L., Nilsson, H., Rubin, M., Simon, W., Wedlund, C., Taylor, M.G.G.T., Vigren, E.: On the origin of molecular oxygen in cometary comae. *Nat. Commun.* **9**(1), 2580 (2018a)
80. Heritier, K.L., Galand, M., Henri, P., Johansson, F.L., Beth, A., Eriksson, A.I., Vallières, X., Altwegg, K., Burch, J.L., Carr, C., Ducrot, E., Hajra, R., Rubin, M.: Plasma source and loss at comet 67P during the Rosetta mission. *A&A* **618**, A77 (2018b). <https://doi.org/10.1093/mnras/stx868>
81. Hilchenbach, M., Fischer, H., Langevin, Y., Merouane, S., Paquette, J., Rynö, J., Stenzel, O., Briois, C., Kissel, J., Koch, A., Schulz, R., Silen, J., Altobelli, N., Baklouti, D., Bardyn, A., Cottin, H., Engrand, C., Fray, N., Haerendel, G., Henkel, H., Höfner, H., Hornung, K., Lehto, H., Mellado, E.M., Modica, P., Roy, L.L., Siljeström, S., Steiger, W., Thirkell, L., Thomas, R., Torkar, K., Varmuza, K., Zaprudin, B.: Mechanical and electrostatic experiments with dust particles collected in the inner coma of comet 67p by cosima onboard rosetta. *Philoso. Trans. R. Soc. A Math. Phys. Eng. Sci.* **375**(2097), 20160255 (2017). <https://doi.org/10.1093/mnras/stx868>
82. Huang, Z., Tóth, G., Gombosi, T.I., Jia, X., Combi, M.R., Hansen, K.C., Fougere, N., Shou, Y., Tenishev, V., Altwegg, K., Rubin, M.: Hall effect in the coma of 67P/Churyumov-Gerasimenko. *MNRAS* **475**(2), 2835–2841 (2018). <https://doi.org/10.1093/mnras/stx3350>, arXiv:1801.03991
83. Ip, W.H., Mendis, D.A.: The flute instability as the trigger mechanism for disruption of cometary plasma tails. *Astrophys. J.* **223**, 671–673 (1978). <https://doi.org/10.1093/mnras/stx868>
84. Johansson, F.L., Odelstad, E., Paulsson, J.J.P., Harang, S.S., Eriksson, A.I., Mannel, T., Vigren, E., Edberg, N.J.T., Miloch, W.J., Simon Wedlund, C., Thiemann, E., Eparvier, F., Andersson, L.: Rosetta photoelectron emission and solar ultraviolet flux at comet 67p. *Mon. Notices Royal Astron. Soc.* **469**(Suppl.2), S626–S635 (2017). <https://doi.org/10.1093/mnras/stx868>
85. Johlander, A., Vaivads, A., Khotyaintsev, Y.V., Gingell, I., Schwartz, S.J., Giles, B.L., Torbert, R.B., Russell, C.T.: Shock ripples observed by the MMS spacecraft: ion reflection and dispersive properties. *Plasma Phys. Control. Fusion* **60**(12), 125006 (2018). <https://doi.org/10.1093/mnras/stx868>
86. Johnson, R.E.: Sputtering and desorption from icy surfaces. In: Schmitt, B., De Bergh, C., Festou, M. (eds.) *Solar System Ices: Based on Reviews Presented at the International Symposium “Solar System Ices” Held in Toulouse, France, on March 27–30, vol. 1995*, pp. 303–334. Springer, Dordrecht (1998). <https://doi.org/10.1093/mnras/stx868>
87. Johnstone, A.D., Coates, A.J., Huddleston, D.E., Jockers, K., Wilken, B., Borg, H., Gurgiolo, C., Winningham, J.D., Amata, E.: Observations of the solar wind and cometary ions during the encounter between Giotto and comet grigg-Skjellerup. *Astron. Astrophys.* **273** (1993)
88. Jones, G.H., Balogh, A., Horbury, T.S.: Identification of comet Hyakutake’s extremely long ion tail from magnetic field signatures. *Nature* **404**(6778), 574–576 (2000). <https://doi.org/10.1093/mnras/stx868>
89. Karlsson, T., Eriksson, A.I., Odelstad, E., André, M., Dickeli, G., Kullen, A., Lindqvist, P.A., Nilsson, H., Richter, I.: Rosetta measurements of lower hybrid frequency range electric field oscillations in the plasma environment of comet 67P. *Geophys. Res. Lett.* **44**, 1641–1651 (2017). <https://doi.org/10.1093/mnras/stx868>



90. Kempf, S., Beckmann, U., Moragas-Klostermeyer, G., Postberg, F., Srama, R., Economou, T., Schmidt, J., Spahn, F., Grün, E.: The E ring in the vicinity of Enceladus. I. Spatial distribution and properties of the ring particles. *Icarus* **193**, 420–437 (2008). <https://doi.org/10.1093/mnras/stx868>
91. Kempf, Y., Pokhotelov, D., Gutynska, O., Wilson, L.B.I.I.I., Walsh, B.M., von Alfthan, S., Hanuuskela, O., Sibeck, D.G., Palmroth, M.: Ion distributions in the Earth's foreshock: Hybrid-Vlasov simulation and THEMIS observations. *JGeophysRes (Space Physics)* **120**, 3684–3701 (2015). <https://doi.org/10.1093/mnras/stx868>
92. Kirkwood, S., Nilsson, H.: High-latitude sporadic-e and other thin layers – the role of magnetospheric electric fields. *Space Sci. Rev.* **91**(3), 579–613 (2000). <https://doi.org/10.1023/A:1005241931650>
93. Koenders, C., Glassmeier, K.H., Richter, I., Motschmann, U., Rubin, M.: Revisiting cometary bow shock positions. *Planet. Space Sci.* **87**, 85–95 (2013). <https://doi.org/10.1093/mnras/stx868>
94. Koenders, C., Perschke, C., Goetz, C., Richter, I., Motschmann, U., Glassmeier, K.H.: Low-frequency waves at comet 67P/Churyumov-Gerasimenko. Observations compared to numerical simulations. *A&A* **594**, A66 (2016). <https://doi.org/10.1093/mnras/stx868>
95. Kurth, W.S., Averkamp, T.F., Gurnett, D.A., Wang, Z.: Cassini RPWS observations of dust in Saturn's E Ring. *Planet. Space Sci.* **54**, 988–998 (2006). <https://doi.org/10.1093/mnras/stx868>
96. Lai, S.T.: A review of critical ionization velocity. *Rev. Geophys.* **39**(4), 471–506 (2001). <https://doi.org/10.1093/mnras/stx868>
97. Lindkvist, J., Hamrin, M., Gunell, H., Nilsson, H., Simon Wedlund, C., Kallio, E., Mann, I., Pitkänen, T., Karlsson, T.: Energy conversion in cometary atmospheres hybrid modeling of 67P/Churyumov-Gerasimenko. *Astron. Astrophys.* **616**, A81 (2018). <https://doi.org/10.1093/mnras/stx868>
98. Lisse, C.M., Dannerl, K., Englhauser, J., Harden, M., Marshall, F.E., Mumma, M.J., Petre, R., Pye, J.P., Ricketts, M.J., Schmitt, J., Trumper, J., West, R.G.: Discovery of x-ray and extreme ultraviolet emission from comet C/Hyakutake 1996 B2. *Science* **274**, 205–209 (1996). <https://doi.org/10.1093/mnras/stx868>
99. Luehr, H., Kloecker, N., Acuña, M.H.: The diamagnetic effect during AMPTE's tail releases - Initial results. *Adv. Space Res.* **8**, 11–14 (1988). <https://doi.org/10.1093/mnras/stx868>
100. Lundin, R., Barabash, S., Andersson, H., Holmström, M., Grigoriev, A., Yamauchi, M., Sauvaud, J.A., Fedorov, A., Budnik, E., Thocaven, J.J., Winningham, D., Frahm, R., Scherrer, J., Sharber, J., Asamura, K., Hayakawa, H., Coates, A., Linder, D.R., Curtis, C., Hsieh, K.C., Sandel, B.R., Grande, M., Carter, M., Reading, D.H., Koskinen, H., Kallio, E., Riihela, P., Schmidt, W., Säles, T., Kozyra, J., Krupp, N., Woch, J., Luhmann, J., McKenna-Lawler, S., Cerulli-Irelli, R., Orsini, S., Maggi, M., Mura, A., Milillo, A., Roelof, E., Williams, D., Livi, S., Brandt, P., Wurz, P., Bochsler, P.: Solar wind-induced atmospheric erosion at Mars: First results from ASPERA-3 on Mars express. *Science* **305**, 1933–1936 (2004). <https://doi.org/10.1093/mnras/stx868>
101. Madanian, H., Cravens, T.E., Burch, J., Goldstein, R., Rubin, M., Nemeth, Z., Goetz, C., Koenders, C., Altwegg, K.: Plasma environment around comet 67P/Churyumov-Gerasimenko at perihelion: Model comparison with rosetta data. *AJ* **153**, 30 (2017). <https://doi.org/10.1093/mnras/stx868>
102. Madsen, B., Simon, Wedlund, C., Eriksson, A., Goetz, C., Karlsson, T., Gunell, H., Spicher, A., Henri, P., Vallières, X., Miloch, W.J.: Extremely low-frequency waves inside the diamagnetic cavity of comet 67P/Churyumov-Gerasimenko. *Geophys. Res. Lett.* **45**, 3854–3864 (2018). <https://doi.org/10.1029/2017GL076415>
103. Mannel, T., Bentley, M., Boakes, P., Jeszenszky, H., Ehrenfreund, P., Engrand, C., Koeberl, C., Levasseur-Regourd, A., Romstedt, J., Schmied, R., Torkar, K., Weber, I.: Dust of comet 67p/churyumov-gerasimenko collected by rosetta/midas: classification and extension to the nanometer scale. *A&A*. <https://doi.org/10.1051/0004-6361/201834851> (2019)
104. Masunaga, K., Nilsson, H., Behar, E., Stenberg Wieser, G., Wieser, M., Goetz, C.: Flow pattern of accelerated cometary ions inside and outside the diamagnetic cavity of comet 67P/Churyumov-Gerasimenko. *A&A* (2019)
105. Mazelle, C., Winterhalter, D., Sauer, K., Trotignon, J.G., Acuña, M.H., Baumgärtel, K., Bertucci, C., Brain, D.A., Brecht, S.H., Delva, M., Dubinin, E., Øieroset, M., Slavin, J.: Bow shock and upstream phenomena at Mars. *Space Sci. Rev.* **111**, 115–181 (2004). <https://doi.org/10.1023/B:SPAC.0000032717.98679.d0>
106. McComas, D.J., Allegrini, F., Bochsler, P., Bzowski, M., Collier, M., Fahr, H., Fichtner, H., Frisch, P., Funsten, H.O., Fuselier, S.A., Gloeckler, G., Gruntman, M., Izmodenov, V., Knappenberger, P., Lee, M., Livi, S., Mitchell, D., Möbius, E., Moore, T., Pope, S., Reisenfeld, D., Roelof, E., Scherrer,

- J., Schwadron, N., Tyler, R., Wieser, M., Witte, M., Wurz, P., Zank, G.: IBEX—interstellar boundary explorer. *Space Sci. Rev.* **146**, 11–33 (2009). <https://doi.org/10.1093/mnras/stx868>
107. Meier, P., Glassmeier, K.H., Motschmann, U.: Modified ion-Weibel instability as a possible source of wave activity at Comet 67P/Churyumov-Gerasimenko. *Annales Geophysicae* **34**(9), 691–707 (2016). <https://doi.org/10.1093/mnras/stx868>
  108. Mendis, D.A., Horányi, M.: Dusty plasma effects in comets: Expectations for rosetta. *Rev. Geophys.* <https://doi.org/10.1093/mnras/stx868> (2013)
  109. Merlino, R.L.: Current-driven dust ion-acoustic instability in a collisional dusty plasma. *IEEE Trans. Plasma Sci.* **25**, 60–65 (1997)
  110. Morooka, M.W., Wahlund, J.E., Eriksson, A.I., Farrell, W.M., Gurnett, D.A., Kurth, W.S., Persoon, A.M., Shafiq, M., André, M., Holmberg, M.K.G.: Dusty plasma in the vicinity of Enceladus. *J. Geophys. Res.* **116**(A12), A12221 (2011). <https://doi.org/10.1093/mnras/stx868>
  111. Nemeth, Z., Burch, J., Goetz, C., Goldstein, R., Henri, P., Koenders, C., Madanian, H., Mandt, K., Mokashi, P., Richter, I., Timar, A., Szego, K.: Charged particle signatures of the diamagnetic cavity of comet 67P/Churyumov-Gerasimenko. *MNRAS* **462**, S415–S421 (2016). <https://doi.org/10.1093/mnras/stx868>
  112. Neubauer, F.M.: Giotto magnetic-field results on the boundaries of the pile-up region and the magnetic cavity. *A&A* **187**, 73–79 (1987)
  113. Neubauer, F.M., Glassmeier, K.H., Pohl, M., Raeder, J., Acuña, M.H., Burlaga, L.F., Ness, N.F., Musmann, G., Mariani, F., Wallis, M.K., Ungstrup, E., Schmidt, H.U.: First results from the Giotto magnetometer experiment at comet Halley. *Nature* **321**, 352–355 (1986). <https://doi.org/10.1093/mnras/stx868>
  114. Neubauer, F.M., Glassmeier, K.H., AJ Coates, A.J., Johnstone, A.D.: Low-frequency electromagnetic plasma waves at comet p/grigg-Skjellerup analysis and interpretation. *J. Geophys. Res.* **98**(A12), 20937–20954 (1993). <https://doi.org/10.1093/mnras/stx868>
  115. Neugebauer, M., Gloeckler, G., Gosling, J.T., Rees, A., Skoug, R., Goldstein, B.E., Armstrong, T.P., Combi, M.R., Mäkinen, T., McComas, D.J., von Steiger, R., Zurbuchen, T.H., Smith, E.J., Geiss, J., Lanzerotti, L.J.: Encounter of the Ulysses spacecraft with the ion tail of comet MCNaught. *ApJ* **667**(2), 1262–1266 (2007). <https://doi.org/10.1093/mnras/stx868>
  116. Niedner, M.B., Ionson, J.A., Brandt, J.C.: Interplanetary gas. XXVI - on the reconnection of magnetic fields in cometary ionospheres at interplanetary sector boundary crossings. *ApJ* **245**, 1159–1169 (1981). <https://doi.org/10.1093/mnras/stx868>
  117. Nilsson, H., Stenberg, W., Wieser, G., Behar, E., Simon, W., Wedlund, C., Gunell, H., Yamauchi, M., Lundin, R., Barabash, S., Wieser, M., Carr, C., Cupido, E., Burch, J.L., Fedorov, A., Sauvaud, J.A., Koskinen, H., Kallio, E., Lebreton, J.P., Eriksson, A., Edberg, N., Goldstein, R., Henri, P., Koenders, C., Mokashi, P., Nemeth, Z., Richter, I., Szego, K., Volwerk, M., Vallat, C., Rubin, M.: Birth of a comet magnetosphere: A spring of water ions. *Science* **347**(1), aaa0571 (2015). <https://doi.org/10.1126/science.aaa0571>
  118. Nilsson, H., Stenberg, W., Wieser, G., Behar, E., Gunell, H., Galand, M., Simon, W., Wedlund, C., Alho, M., Goetz, C., Yamauchi, M., Henri, P., Eriksson, E.O.A.: Evolution of the ion environment of comet 67P, during the rosetta mission as seen by RPC-ICA. *Mon. Notices R. Astron. Soc.* **469**(Suppl.2), S252–S261 (2017). <https://doi.org/10.1093/mnras/stx868>
  119. Nilsson, H., Gunell, H., Karlsson, T., Brenning, N., Henri, P., Goetz, C., Eriksson, A.I., Behar, E., Stenberg, W., Vallières, X.: Size of a plasma cloud matters: The polarisation electric field of a small-scale comet ionosphere. *Astron. Astrophys.* **616**, A50 (2018). <https://doi.org/10.1093/mnras/stx868>
  120. Noonan, J.W., Stern, S.A., Feldman, P.D., Broiles, T., Simon, W., Wedlund, C., Edberg, N.J.T., Schindhelm, E., Parker, J.W., Keeney, B.A., Vervack, R.J. Jr., Steffl, A.J., Knight, M.M., Weaver, H.A., Feaga, L.M., A'Hearn, M., Bertaux, J.L.: Ultraviolet observations of coronal mass ejection impact on comet 67P /Churyumov-Gerasimenko by Rosetta Alice. *AJ* **156**, 16 (2018). <https://doi.org/10.1093/mnras/stx868>
  121. Odelstad, E., Eriksson, A.I., Johansson, F.L., Vigren, E., Henri, P., Gilet, N., Heritier, K.L., Vallières, X., Rubin, M., André, M.: Ion velocity and electron temperature inside and around the diamagnetic cavity of comet 67P. *J. Geophys. Res. Space Phys.* **123**(7), 5870–5893 (2018). <https://doi.org/10.1093/mnras/stx868>
  122. Oya, H., Morioka, A., Miyake, W., Smith, E.J., Tsurutani, B.T.: Discovery of cometary kilometric radiations and plasma waves at comet Halley. *Nature* **321**, 307–310 (1986). <https://doi.org/10.1093/mnras/stx868>




123. Plaschke, F., Hietala, H., Archer, M., Blanco-Cano, X., Kajdič, P., Karlsson, T., Lee, S.H., Omid, N., Palmroth, M., Roytershteyn, V., Schmid, D., Sergeev, V., Sibeck, D.: Jets downstream of collisionless shocks. *Space Sci. Rev.* **214**(5), 81 (2018). <https://doi.org/10.1093/mnras/stx868>
124. Rahe, J.: The structure of tail rays in the coma region of comets. *Zeitschr Astrophys.* **68**, 208–213 (1968)
125. Rahe, J., Donn, B.: Ionization and ray formation in comets. *Astron. J.* **74**, 256–258 (1969)
126. Richter, I., Koenders, C., Auster, H.U., Frühauff, D., Götz, C., Heinisch, P., Perschke, C., Motschmann, U., Stoll, B., Altwegg, K., Burch, J., Carr, C., Cupido, E., Eriksson, A., Henri, P., Goldstein, R., Lebreton, J.P., Mokashi, P., Nemeth, Z., Nilsson, H., Rubin, M., Szegő, K., Tsurutani, B.T., Vallat, C., Volwerk, M., Glassmeier, K.H.: Observation of a new type of low-frequency waves at comet 67P/Churyumov-Gerasimenko. *Annales Geophysicae* **33**, 1031–1036 (2015). <https://doi.org/10.5194/angeo-33-1031-2015>, arXiv:1505.06068
127. Richter, I., Auster, H.U., Berghofer, G., Carr, C., Cupido, E., Fornaçon, K.H., Goetz, C., Heinisch, P., Koenders, C., Stoll, B., Tsurutani, B.T., Vallat, C., Volwerk, M., Glassmeier, K.H.: Two-point observations of low-frequency waves at 67P/Churyumov-Gerasimenko during the descent of PHILAE: comparison of RPCMAG and ROMAP. *Annales Geophysicae* **34**, 609–622 (2016). <https://doi.org/10.1093/mnras/stx868>
128. Riedler, W., Schwingenschuh, K., Yeroshenko, Y.E., Styashkin, V.A., Russell, C.T.: Magnetic field observations in comet Halley's coma. *Nature* **321**, 288–289 (1986). <https://doi.org/10.1093/mnras/stx868>
129. Rubin, M., Hansen, K.C., Combi, M.R., Daldorff, L.K.S., Gombosi, T.I., Tenishev, V.M.: Kelvin-helmholtz instabilities at the magnetic cavity boundary of comet 67P/Churyumov-Gerasimenko. *J. Geophys. Res. (Space Phys)* **117**, A06227 (2012). <https://doi.org/10.1093/mnras/stx868>
130. Sauer, K., Baumgaertel, K.: Magnetic cavity formation at comet Halley and at the AMPTE Li release. In: Rolfe, E.J., Battrick, B., Ackerman, M., Scherer, M., Reinhard, R. (eds.) *Diversity and Similarity of Comets*, vol. 278, pp. 113–118 (1987)
131. Scarf, F.: Plasma wave observations at Comets giacobini-Zinner and Halley. Washington DC Am. Geophys. Union Geophys. Monograph. Ser. **53**, 31–40 (1989)
132. Scarf, F.L., Ferdinand, V., Coroniti, V., Kennel, C.F., Gurnett, D.A., Ip, W.H., Smith, E.J.: Plasma wave observations at comet giacobini-Zinner. *Science* **232**, 377–381 (1986). <https://doi.org/10.1093/mnras/stx868>
133. Schaible, M.J., Dukes, C.A., Hutcherson, A.C., Lee, P., Collier, M.R., Johnson, R.E.: Solar wind sputtering rates of small bodies and ion mass spectrometry detection of secondary ions. *J. Geophys. Res. (Planets)* **122**, 1968–1983 (2017). <https://doi.org/10.1093/mnras/stx868>
134. Schillings, A., Nilsson, H., Slapak, R., Wintoft, P., Yamauchi, M., Wik, M., Dandouras, I., Carr, C.M.: O<sup>+</sup> escape during the extreme space weather event of 4–10 September 2017. *Space Weather* **16**(9), 1363–1376 (2018). <https://doi.org/10.1093/mnras/stx868>
135. Shan, L., Lu, Q., Mazelle, C., Huang, C., Zhang, T., Wu, M., Gao, X., Wang, S.: The shape of the Venusian bow shock at solar minimum and maximum: Revisit based on VEX observations. *PlanetSpaceSci* **109**, 32–37 (2015). <https://doi.org/10.1093/mnras/stx868>
136. Simon Wedlund C, Kallio, E., Alho, M., Nilsson, H., Stenberg Wieser, G., Gunell, H., Behar, E., Pusa, J., Gronoff, G.: The atmosphere of comet 67P/Churyumov-Gerasimenko diagnosed by charge-exchanged solar wind alpha particles. *A&A* **587**, A154 (2016). <https://doi.org/10.1093/mnras/stx868>
137. Simon Wedlund C, Alho, M., Gronoff, G., Kallio, E., Gunell, H., Nilsson, H., Lindkvist, J., Behar, E., Stenberg Wieser, G., Miloch, W.J.: Hybrid modelling of cometary plasma environments. I. Impact of photoionisation, charge exchange, and electron ionisation on bow shock and cometopause at 67P/Churyumov-Gerasimenko. *A&A* **604**, A73 (2017). <https://doi.org/10.1093/mnras/stx868>
138. Simon Wedlund C, Behar, E., Kallio, E., Nilsson, H., Alho, M., Gunell, H., Bodewits, D., Beth, A., Gronoff, G., Hoekstra, R.: Solar wind charge exchange in cometary atmospheres. II. Analytical model. *Astron. Astrophys.* <https://doi.org/10.1093/mnras/stx868> (2019)
139. Simon Wedlund C, Behar, E., Nilsson, H., Alho, M., Kallio, E., Gunell, H., Bodewits, D., Heritier, K., Galand, M., Beth, A., Rubin, M., Altwegg, K., Volwerk, M., Gronoff, G., Hoekstra, R.: Solar wind charge exchange in cometary atmospheres. III. Results from the Rosetta mission to comet 67P/Churyumov-Gerasimenko. *Astron. Astrophys.* **630**, A37 (2019). <https://doi.org/10.1051/0004-6361/201834881>, arXiv:1902.04417

140. Simon Wedlund C, Bodewits, D., Alho, M., Hoekstra, R., Behar, E., Gronoff, G., Gunell, H., Nilsson, H., Kallio, E., Beth, A.: Solar wind charge exchange in cometary atmospheres. I. Charge-changing and ionization cross sections for he and h particles in H<sub>2</sub>O. *Astron. Astrophys.* (2019)
141. Slavin, J.A., Smith, E.J., Tsurutani, B.T., Siscoe, G.L., Jones, D.E., Mendis, D.A.: Giacobini-zinner magnetotail - ICE magnetic field observations. *Geophys. Res. Lett.* **13**, 283–286 (1986). <https://doi.org/10.1093/mnras/stx868>
142. Smith, E.J., Tsurutani, B.T., Slavin, J.A., Jones, D.E., Siscoe, G.L., Mendis, D.A.: International cometary explorer encounter with giacobini-Zinner: Magnetic field observations. *Science* **232**(4748), 382–385 (1986). <https://doi.org/10.1093/mnras/stx868>
143. Szegő, K., Glassmeier, K.H., Bingham, R., Bogdanov, A., Fischer, C., Haerendel, G., Brinca, A., Cravens, T., Dubinin, E., Sauer, K., Fisk, L., Gombosi, T., Schwadron, N., Isenberg, P., Lee, M., Mazelle, C., Möbius, E., Motschmann, U., Shapiro, V.D., Tsurutani, B., Zank, G.: Physics of mass loaded plasmas. *Space Sci Rev* **94**, 429–671 (2000)
144. Tsurutani, B.T.: Comets: a laboratory for plasma waves and instabilities. Washington DC Am. Geophys. Union Geophys. Monograph. Ser. **61**, 189–209 (1991)
145. Tsurutani, B.T., Lakhina, G.S., Smith, E.J., Buti, B., Moses, S.L., Coroniti, F.V., Brinca, A.L., Slavin, J.A., Zwickl, R.D.: Mirror mode structures and elf plasma waves in the giacobini-Zinner magnetosheath. *Nonlinear Process. Geophys.* **6**, 229–234 (1999). <https://doi.org/10.1093/mnras/stx868>
146. Valenzuela, A., Haerendel, G., Föppl, H., Melzner, F., Neuss, H., Rieger, E., Stöcker, J., Bauer, O., Höfner, H., Loidl, J.: The AMPTE artificial comet experiments. *Nature* **320**, 700–703 (1986). <https://doi.org/10.1093/mnras/stx868>
147. Verscharen, D., Wicks, R.T., Branduardi-Raymont, G., Erdélyi, R., Frontera, F., Götz, C., Guidorzi, C., Leboutteiller, V., Matthews, S.A., Nicastro, F., Rae, I.J., Retinò, A., Simionescu, A., Soffitta, P., Uttley, P., Wimmer-Schweingruber, R.F.: The plasma universe: a coherent science theme for voyage 2050. *Front. Astron. Space Sci.* **8**, 30 (2021). <https://doi.org/10.3389/fspas.2021.651070>, arXiv:2104.07983
148. Vigren, E., Eriksson, A.I.: A 1D model of radial ion motion interrupted by Ion-Neutral interactions in a cometary coma. *AJ* **153**, 150 (2017). <https://doi.org/10.1093/mnras/stx868>
149. Vigren, E., Galand, M.: Predictions of ion production rates and ion number densities within the diamagnetic cavity of comet 67P/Churyumov-Gerasimenko at perihelion. *ApJ* **772**, 33 (2013). <https://doi.org/10.1093/mnras/stx868>
150. Vigren, E., Galand, M., Lavvas, P., Eriksson, A.I., Wahlund, J.E.: On the possibility of significant electron depletion due to nanograin charging in the coma of comet 67P/Churyumov-Gerasimenko near perihelion. *Ap J* **798**, 130 (2015). <https://doi.org/10.1093/mnras/stx868>
151. Vigren, E., André, M., Edberg, N.J.T., Engelhardt, I.A.D., Eriksson, A.I., Galand, M., Goetz, C., Henri, P., Heritier, K., Johansson, F.L., Nilsson, H., Odelstad, E., Rubin, M., Stenberg-Wieser, G., Tzou, C.Y., Vallières, X.: Effective ion speeds at 200–250 km from comet 67P/Churyumov-Gerasimenko near perihelion. *MNRAS* **469**, S142–S148 (2017). <https://doi.org/10.1093/mnras/stx868>
152. Vourlidas, A., Davis, C.J., Eyles, C.J., Crothers, S.R., Harrison, R.A., Howard, R.A., Moses, J.D., Socker, D.G.: First direct observation of the interaction between a comet and a coronal mass ejection leading to a complete plasma tail disconnection. *ApJ* **668**, L79–L82 (2007). <https://doi.org/10.1093/mnras/stx868>
153. Wargelin, B., Beiersdorfer, P., Brown, G.: Ebit charge-exchange measurements and astrophysical applications. *Can. J. Phys.* **86**(1), 151–169 (2008). <https://doi.org/10.1093/mnras/stx868>
154. Wegmann, R.: MHD Model calculations for the effect of interplanetary shocks on the plasma tail of a comet. *A&A* **294**, 601–614 (1995)
155. Wurz, P., Rubin, M., Altwegg, K., Balsiger, H., Berthelier, J.J., Bieler, A., Calmonte, U., De Keyser, J., Fiethe, B., Fuselier, S., Galli, A., Gasc, S., Gombosi, T.I., Jäckel, A., Le Roy, L., Mall, U.A., Rème, H., Tennishev, V., Tzou, C.Y.: Solar wind sputtering of dust on the surface of 67p/churyumov-gerasimenko. *A&A* **583**, A22 (2015). <https://doi.org/10.1093/mnras/stx868>
156. Yao, Y., Giapis, K.P.: Dynamic molecular oxygen production in cometary comae. *Nat. Commun.* **8**, 15298 EP – (2017)
157. Yumoto, K., Saito, T., Nakagawa, T.: Hydromagnetic waves near O<sup>+</sup> (or H<sub>2</sub>O<sup>+</sup>) ion cyclotron frequency observed by Sakigake at the closest approach to comet Halley. *Geophys. Res. Lett.* **13**(8), 825–828 (1986). <https://doi.org/10.1093/mnras/stx868>

158. Zhang, T.L., Delva, M., Baumjohann, W., Volwerk, M., Russell, C.T., Wei, H.Y., Wang, C., Balikhin, M., Barabash, S., Auster, H.U., Kudela, K.: Induced magnetosphere and its outer boundary at Venus. *JGeophysRes (Planets)* **113**, E00B20 (2008). <https://doi.org/10.1029/2008JE003215>
159. Ziegler, J.F.: SRIM-2003. *Nucl. Instrum. Methods Phys. Res. B* **219**, 1027–1036 (2004). <https://doi.org/10.1093/mnras/stx868>

**Publisher's note** Springer Nature remains neutral with regard to jurisdictional claims in published maps and institutional affiliations.

## Affiliations

C. Goetz<sup>1,2</sup>  · H. Gunell<sup>3</sup> · M. Volwerk<sup>4</sup> · A. Beth<sup>5</sup> · A. Eriksson<sup>6</sup> · M. Galand<sup>5</sup> · P. Henri<sup>7</sup> · H. Nilsson<sup>8</sup> · C. Simon Wedlund<sup>4</sup> · M. Alho<sup>9</sup> · L. Andersson<sup>10</sup> · N. Andre<sup>11</sup> · J. De Keyser<sup>12</sup> · J. Deca<sup>10</sup> · Y. Ge<sup>13</sup> · K.-H. Glassmeier<sup>14</sup> · R. Hajra<sup>15</sup> · T. Karlsson<sup>16</sup> · S. Kasahara<sup>17</sup> · I. Kolmasova<sup>18,19</sup> · K. LLera<sup>20</sup> · H. Madanian<sup>20</sup> · I. Mann<sup>21</sup> · C. Mazelle<sup>11</sup> · E. Odelstad<sup>16</sup> · F. Plaschke<sup>4</sup> · M. Rubin<sup>22</sup> · B. Sanchez-Cano<sup>23</sup> · C. Snodgrass<sup>24</sup> · E. Vigren<sup>6</sup>

<sup>1</sup> IGeP, TU Braunschweig, Brunswick, Germany

<sup>2</sup> ESA-ESTEC, Noordwijk, Netherlands

<sup>3</sup> Umeå Universitet, Umeå, Sweden

<sup>4</sup> Space Research Institute, Austrian Academy of Sciences, Graz, Austria

<sup>5</sup> Imperial College London, London, UK

<sup>6</sup> IRF Uppsala, Uppsala, Sweden

<sup>7</sup> LPC2E, CNRS, Orleans, France

<sup>8</sup> IRF Kiruna, Kiruna, Sweden

<sup>9</sup> Aalto University, Espoo, Finland

<sup>10</sup> LASP, University of Colorado, Boulder, CO, USA

<sup>11</sup> IRAP, Toulouse, France

<sup>12</sup> Royal Belgian Institute for Space Aeronomy, Brussels, Belgium

<sup>13</sup> Chinese Academy of Sciences, Beijing, China

<sup>14</sup> TU Braunschweig, Brunswick, Germany

<sup>15</sup> National Atmospheric Research Laboratory, Tirupati, India

<sup>16</sup> KTH Stockholm, Stockholm, Sweden

<sup>17</sup> University of Tokyo, Tokyo, Japan

<sup>18</sup> Department of Space Physics, Institute of Atmospheric Physics of the Czech Academy of Sciences, Prague, Czechia

<sup>19</sup> Faculty of Mathematics and Physics, Charles University, Prague, Czechia

<sup>20</sup> Southwest Research Institute, San Antonio, TX, USA

<sup>21</sup> UiT, The Arctic University of Norway, Tromsø, Norway

<sup>22</sup> Universität Bern, Bern, Switzerland

<sup>23</sup> University of Leicester, Leicester, UK

<sup>24</sup> University of Edinburgh, Edinburgh, UK